

CHAPTER 8

PHARMACOKINETICS AND BIODISTRIBUTION STUDIES

8 PHARMACOKINETICS AND BIODISTRIBUTION STUDIES

8.1 Introduction

Assessment of biodistribution of drugs and drug delivery system is very important to understand the fate of delivery system *in-vivo*. In last few years, radiolabelling has also been used to recognize the biodistribution of various delivery systems. Reports from the literature indicated the usefulness of radiolabeled formulation to study biodistribution and scintigraphy imaging in animals. The surface properties of particular carriers greatly define their *in vivo* fate. The extent and nature of opsonin adsorption at the surface of colloidal particles and their simultaneous blood clearance depend on the physicochemical properties of the particles such as size, surface charge and surface hydrophobicity (Jaeghere et al., 1999).

8.2 Methods

8.2.1 Animals

All experiments conducted on animals were approved by the Social Justice and Empowerment Committee, for the purpose of control and supervision on animals and experiments, Ministry of Government of India. The tissue biodistribution study was carried out in healthy swiss mice weighing between 25 to 30 g.

8.2.2 Pharmacokinetics and Biodistribution Studies of Nanoparticles

Three mice were used at each time point for each nanoparticles (NPs) formulation. The mice were divided into four groups for each drug, Tramadol (TMD) and Lamotrigine (LTG). Group I, group II, group III and group IV were administered ^{99m}Tc -TMDS, ^{99m}Tc -TMD-NPs, ^{99m}Tc -Tf-TMD-NPs and ^{99m}Tc -Lf-TMD-NPs respectively. Similarly for LTG, Group I, group II, group III and group IV were administered ^{99m}Tc -TMDS, ^{99m}Tc -LTG-NPs, ^{99m}Tc -Tf-LTG-NPs and ^{99m}Tc -Lf-LTG-NPs respectively. Solutions (TMDS and LTGS) were used for comparative evaluation. All groups received 74-88.8 MBq/kg of radioactivity administered intravenously (100 μ l) via tail vein. The mice were sacrificed at different time intervals of 0.17, 0.5, 1, 2, 4, 24 and 48 h and blood was collected via cardiac puncture. Different organs including brain, liver, spleen, kidney, lungs and heart were dissected, washed twice with normal saline, made free from any adhering tissues, dried between adsorbent paper-folds, placed in pre-weighed plastic tubes, and weighed. The radioactivity present in each tissue/organ was determined using shielded well-type gamma scintillation counter along with 3 samples of standard solution representing 100% of the administered dose. The radioactivity

in each organ/tissue was determined as fraction of administered dose per gram of the tissue (%A/g).

$$\%A/g = \frac{\text{Sample count}}{\text{Sample weight} \times \text{Standard count}} \times 100$$

The radioactivities determined included the delivery system in the vascular space as well as in the tissue parenchyma. Hence a correction was made for the radioactivity in the vascular space using the following formula as reported (Hatakeyama K et al., 2004).

$$X_{\text{tissue}} = X_{\text{organ}} - V_0 C_{(t)}$$

Where V_0 denotes the total volume of the vascular space and interstitial fluid, as determined by the radioactivities in the whole organ samples divided by the blood concentration 10 min after iv injection.

The results of radioactivity measured for TMD formulations administered by intravenous route at various time points in different organs are recorded in Table 8.1, 8.2, 8.3 and 8.4 for ^{99m}Tc -TMDS, ^{99m}Tc -TMD-NPs, ^{99m}Tc -Tf-TMD-NPs and ^{99m}Tc -Lf-TMD-NPs respectively. The blood concentration of TMD formulations vs. time are plotted in Fig. 8.1. Fig. 8.2 represents the brain concentrations of TMD formulations vs. time profile. TMD concentration in different organ at various time points is plotted in Fig. 8.3. The results of radioactivity measured for LTG formulations at various time points in different organs are recorded in Table 8.9, 8.10, 8.11 and 8.12 for ^{99m}Tc -LTGS, ^{99m}Tc -LTG-NPs, ^{99m}Tc -Tf-LTG-NPs and ^{99m}Tc -Lf-LTG-NPs respectively. The blood concentrations of LTG formulations vs. time (h) are plotted in Fig. 8.4. Fig. 8.5 represents the brain concentrations of LTG formulations vs. time profile. LTG concentration in different organ at various time points is plotted in Fig. 8.6.

Gamma Scintigraphy Studies

Gamma Scintigraphy was done in mice after administering intravenously, 100 μ l of ^{99m}Tc -labeled complexes of TMDS, TMD-NPs and Tf-TMD-NPs containing 5.55 to 6.66 MBq of ^{99m}Tc . The mice were partially anesthetized with diethyl ether and were mount on a wooden board. The imaging was performed on single photon emission computerized tomography (SPECT, LC 75-005, Diacam, Siemens, Hoffman Estates, IL, USA) after 2 h. The gamma scintigraphic image is shown in Fig. 8.7

8.2.3 Pharmacokinetics and Biodistribution Studies of Micro and Nanoemulsion

Three mice were used at each time point for each formulation. The mice were divided into three groups for each drug, TMD and LTG. Group I, group II and group III were administered ^{99m}Tc -TS, ^{99m}Tc -TME and ^{99m}Tc -TNE respectively. Similarly for LTG, Group I, group II and group III were administered ^{99m}Tc -LS, ^{99m}Tc -LME and ^{99m}Tc -LNE respectively. Solutions (TS and LS) were used for comparative evaluation. All groups received 44.4-53.28 MBq/kg of radioactivity incorporated in 10 μL of ^{99m}Tc -TS, ^{99m}Tc -LS, ^{99m}Tc -TNE and ^{99m}Tc -LNE and 8 μL of ^{99m}Tc -TME and ^{99m}Tc -LME, administered via intranasal route. Before nasal administration of the formulations, the mice were partially anesthetized with diethyl ether. 4/5 μL of formulation was administered in the each nostril using micropipette (10 μL) fixed with low density polyethylene tube having 0.10 mm internal diameter at the delivery site. The rats were held from the back in slanted position during nasal administration (Jogani VV et al., 2008).

The mice were sacrificed at different time intervals of 0.5, 1, 2, 4, 24 and 48 h and blood was collected via cardiac puncture. Different organs including brain, liver, spleen, kidney, lungs, stomach and intestine were dissected, washed twice with normal saline, made free from any adhering tissues, dried between adsorbent paper-folds, placed in pre-weighed plastic tubes, and weighed. The radioactivity present in each tissue/organ was determined using shielded well-type gamma scintillation counter along with 3 samples of standard solution representing 100% of the administered dose. The radioactivity in each organ/tissue was determined as fraction of administered dose per gram of the tissue (%A/g). The radioactivities determined included the delivery system in the vascular space as well as in the tissue parenchyma. Hence a correction was made for the radioactivity in the vascular space using the following formula as reported (Hatakeyama K et al., 2004).

$$X_{\text{tissue}} = X_{\text{organ}} - V_0 C_{(t)}$$

Where V_0 denotes the total volume of the vascular space and interstitial fluid, as determined by the radioactivities in the whole organ samples divided by the blood concentration 10 min after iv injection.

The nasal bioavailability of the drugs from the formulations was calculated using equation (Zhao Y et al., 2007).

$$\% \text{ Nasal bioavailability} = \frac{\text{AUC}_{\text{in}}}{\text{AUC}_{\text{iv}}} \times 100$$

To evaluate the brain targeting efficiency, 2 indices [Drug targeting efficiency (DTE) (%) and direct nose-to-brain transport (DTP)(%)] were adopted as mentioned below. (Jung BH et al., 2000; Zhang Q et al., 2004)

Brain targeting efficiency was calculated using two equations mentioned below. Drug targeting efficiency (DTE%) represents time average partitioning ratio.

$$DTE = \frac{AUC_{\text{brain}}}{AUC_{\text{blood}}} \times 100$$

Where, AUC indicates area under the curve.

Brain drug-direct-transport percentage [DTP%] was calculated using equations:

$$DTP = \frac{B_{in} - B_x}{B_{in}} \times 100$$

Where,

$$B_x = \frac{B_{iv}}{P_{iv}} \times P_{in}$$

B_x = Brain AUC fraction contributed by systemic circulation through the blood-brain-barrier (BBB) following intranasal administration.

B_{IV} = $AUC_{0 \rightarrow 24}$ (brain) following intravenous administration.

P_{IV} = $AUC_{0 \rightarrow 24}$ (blood) following intravenous administration.

B_{IN} = $AUC_{0 \rightarrow 24}$ (brain) following intranasal administration.

P_{IN} = $AUC_{0 \rightarrow 24}$ (blood) following intranasal administration.

AUC = Area under the curve.

The results of radioactivity measured for TMD formulations administered by intranasal route at various time points in different organs are recorded in Table 8.17, 8.18 and 8.19 for ^{99m}Tc -TS, ^{99m}Tc -TME and ^{99m}Tc -TNE respectively. The blood concentrations of TMD formulations vs. time (h) are plotted in Fig. 8.8. Fig. 8.9 represents the brain concentrations of TMD formulations vs. time profile. TMD concentration in different organ at various time points is plotted in Fig. 8.10.

The results of radioactivity measured for LTG formulations administered by intranasal route at various time points in different organs are recorded in Table 8.23, 8.24, and 8.25 for ^{99m}Tc -LS, ^{99m}Tc -LME and ^{99m}Tc -LNE respectively. The blood concentrations of LTG formulations

vs. time (h) are plotted in Fig. 8.11. Fig. 8.12 represents the brain concentrations of LTG formulations vs. time profile. LTG concentration in different organ at various time points is plotted in Fig. 8.13.

8.2.4 Statistical Analysis

All data are reported as mean \pm SD (standard deviation). Pharmacokinetic parameters were calculated using Kinetica (version 4.40, Innaphase, Philadelphia, PA, USA) applying non compartmental kinetics for iv bolus for NPs and extra-vascular for ME and NE. Statistical evaluations were compared using ANOVA and differences greater at $p < 0.05$ were considered significant.

8.3 Result and Discussion

8.3.1 Pharmacokinetics and Biodistribution studies of Nanoparticles

The radiolabeled complexes of TMDs, TMD-NPs, Tf-TMD-NPs and Lf-TMD-NPs were evaluated for biodistribution in healthy swiss mice for 48 h after intravenous administration. The results of biodistribution for various radiolabelled complexed formulations are tabulated in table 8.1, 8.2, 8.3, and 8.4. The radiolabeled complexes of LTGS, LTG-NPs, Tf-LTG-NPs and Lf-LTG-NPs were evaluated for biodistribution in healthy swiss mice for 48 h after intravenous administration. The results of biodistribution for various radiolabelled complexed formulations are tabulated in Table 8.9, 8.10, 8.11, and 8.12.

Table 8.1: Tissue / Organ distribution of ^{99m}Tc labelled TMDs

Organ/ Tissue	%A/g					
	0.5h	1h	2h	4h	24h	48h
Blood*	4.35 \pm 0.28	3.11 \pm 0.08	2.12 \pm 0.08	1.31 \pm 0.12	0.13 \pm 0.01	ND
Brain	0.07 \pm 0.01	0.06 \pm 0.004	0.05 \pm 0.002	0.04 \pm 0.003	ND	ND
Liver	56.57 \pm 2.96	48.28 \pm 3.94	28.88 \pm 2.09	10.46 \pm 0.71	1.05 \pm 0.17	0.16 \pm 0.03
Spleen	29.51 \pm 2.22	20.78 \pm 1.63	15.44 \pm 0.53	5.20 \pm 0.47	0.22 \pm 0.03	0.07 \pm 0.03
Kidney	10.92 \pm 1.19	9.93 \pm 0.31	7.76 \pm 0.56	3.52 \pm 0.17	0.16 \pm 0.04	0.04 \pm 0.02
Heart	4.13 \pm 0.61	2.36 \pm 0.18	1.35 \pm 0.15	1.36 \pm 0.10	0.14 \pm 0.06	0.07 \pm 0.03
Lungs	8.75 \pm 1.53	4.89 \pm 1.36	2.55 \pm 0.16	1.45 \pm 0.07	0.18 \pm 0.02	0.02 \pm 0.01
Stomach	0.12 \pm 0.01	0.07 \pm 0.01	0.04 \pm 0.003	0.01 \pm 0.001	ND	ND
Intestine	0.15 \pm 0.02	0.09 \pm 0.02	0.05 \pm 0.002	0.03 \pm 0.001	ND	ND

Values are represented as mean \pm SD, n=3. ND-Not Detected; *0.17h time point for blood was not tabulated

Table 8.2: Tissue / Organ distribution of ^{99m}Tc labelled TMD-NPs

Organ/ Tissue	% A/g					
	0.5h	1h	2h	4h	24h	48h
Blood*	5.67 \pm 0.30	4.50 \pm 0.34	3.39 \pm 0.21	2.08 \pm 0.22	0.75 \pm 0.04	0.30 \pm 0.01
Brain	0.07 \pm 0.01	0.12 \pm 0.02	0.07 \pm 0.01	0.06 \pm 0.003	0.02 \pm 0.01	0.01 \pm 0.001
Liver	15.01 \pm 1.24	14.42 \pm 1.09	10.75 \pm 1.58	6.12 \pm 0.25	1.04 \pm 0.12	0.25 \pm 0.05
Spleen	9.69 \pm 0.99	14.04 \pm 1.00	9.22 \pm 0.88	4.02 \pm 0.21	1.50 \pm 0.06	0.38 \pm 0.09
Kidney	6.59 \pm 0.60	6.94 \pm 0.21	5.48 \pm 0.60	3.05 \pm 0.39	0.31 \pm 0.02	0.05 \pm 0.02
Heart	1.69 \pm 0.17	1.07 \pm 0.15	0.72 \pm 0.12	0.45 \pm 0.06	0.19 \pm 0.02	0.08 \pm 0.02
Lungs	3.93 \pm 0.77	2.47 \pm 0.25	1.38 \pm 0.10	0.72 \pm 0.06	0.35 \pm 0.10	0.11 \pm 0.07

Values are represented as mean \pm SD, n=3; *0.17h time point for blood was not tabulated

Table 8.3: Tissue / Organ distribution of ^{99m}Tc labelled Tf-TMD-NPs

Organ/ Tissue	% A/g					
	0.5h	1h	2h	4h	24h	48h
Blood*	5.54 \pm 0.21	4.27 \pm 0.21	3.43 \pm 0.14	2.09 \pm 0.14	0.72 \pm 0.04	0.25 \pm 0.02
Brain	0.08 \pm 0.01	0.15 \pm 0.04	0.22 \pm 0.03	0.13 \pm 0.01	0.06 \pm 0.01	0.02 \pm 0.001
Liver	17.28 \pm 2.06	18.59 \pm 1.72	13.92 \pm 1.55	6.92 \pm 0.40	1.83 \pm 0.13	0.39 \pm 0.10
Spleen	12.78 \pm 1.58	20.88 \pm 2.07	11.73 \pm 1.00	6.99 \pm 0.80	2.12 \pm 0.21	0.52 \pm 0.08
Kidney	6.56 \pm 0.73	9.59 \pm 0.49	8.24 \pm 0.31	4.14 \pm 0.22	0.45 \pm 0.11	0.11 \pm 0.03
Heart	1.27 \pm 0.23	0.71 \pm 0.15	0.55 \pm 0.06	0.32 \pm 0.11	0.14 \pm 0.05	0.04 \pm 0.02
Lungs	2.72 \pm 0.30	1.57 \pm 0.33	0.95 \pm 0.12	0.40 \pm 0.08	0.27 \pm 0.04	0.06 \pm 0.01

Values are represented as mean \pm SD, n=3; *0.17h time point for blood was not tabulated

Table 8.4: Tissue / Organ distribution of ^{99m}Tc labelled Lf-TMD-NPs

Organ/ Tissue	% A/g					
	0.5h	1h	2h	4h	24h	48h
Blood*	5.38 \pm 0.30	4.13 \pm 0.09	3.36 \pm 0.25	1.90 \pm 0.23	0.68 \pm 0.03	0.19 \pm 0.03
Brain	0.20 \pm 0.03	0.23 \pm 0.04	0.41 \pm 0.07	0.20 \pm 0.01	0.08 \pm 0.01	0.03 \pm 0.001
Liver	17.28 \pm 0.49	21.58 \pm 1.87	15.27 \pm 1.56	9.75 \pm 0.56	2.25 \pm 0.12	0.44 \pm 0.01
Spleen	11.47 \pm 0.70	19.29 \pm 1.38	10.25 \pm 0.68	5.76 \pm 0.23	2.01 \pm 0.09	0.50 \pm 0.03
Kidney	7.35 \pm 0.65	9.12 \pm 0.30	8.02 \pm 0.64	4.93 \pm 0.52	0.37 \pm 0.02	0.09 \pm 0.02
Heart	1.06 \pm 0.08	0.51 \pm 0.10	0.42 \pm 0.07	0.37 \pm 0.09	0.09 \pm 0.02	ND
Lungs	2.58 \pm 0.66	1.41 \pm 0.23	0.93 \pm 0.06	0.52 \pm 0.07	0.25 \pm 0.04	0.07 \pm 0.02

Values are represented as mean \pm SD, n=3; *0.17h time point for blood was not tabulated

Figure 8.1 Pharmacokinetic profiles of ^{99m}Tc labelled TMDS and TMD NPs formulations in blood

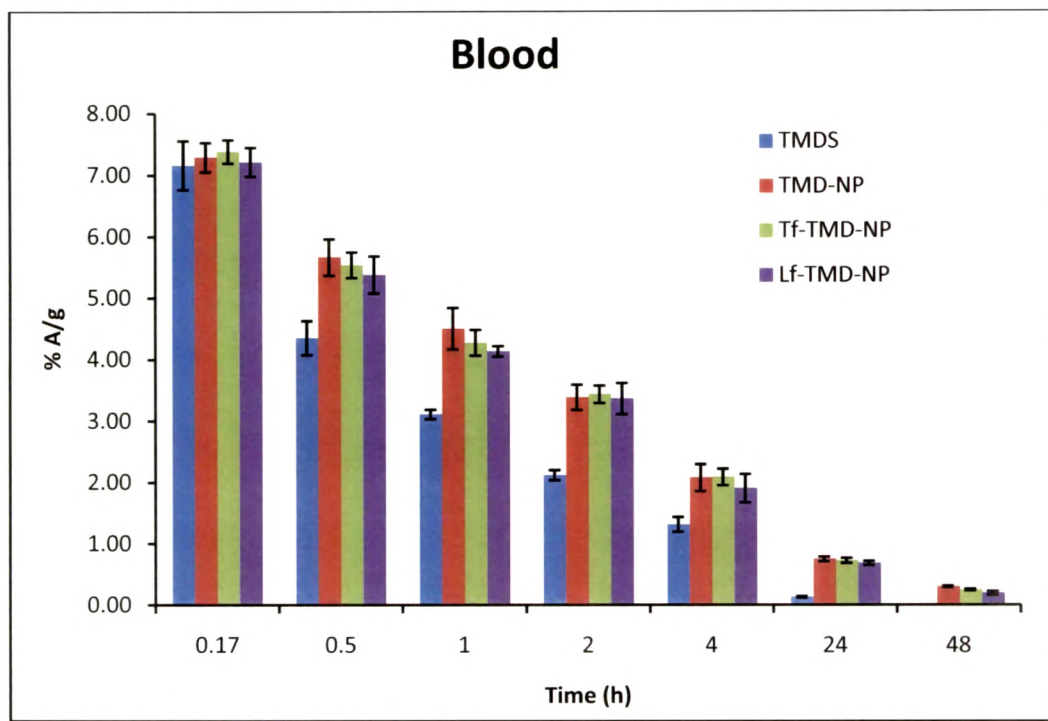


Figure 8.2 Distribution of ^{99m}Tc labelled TMDS and TMD NPs formulations in brain

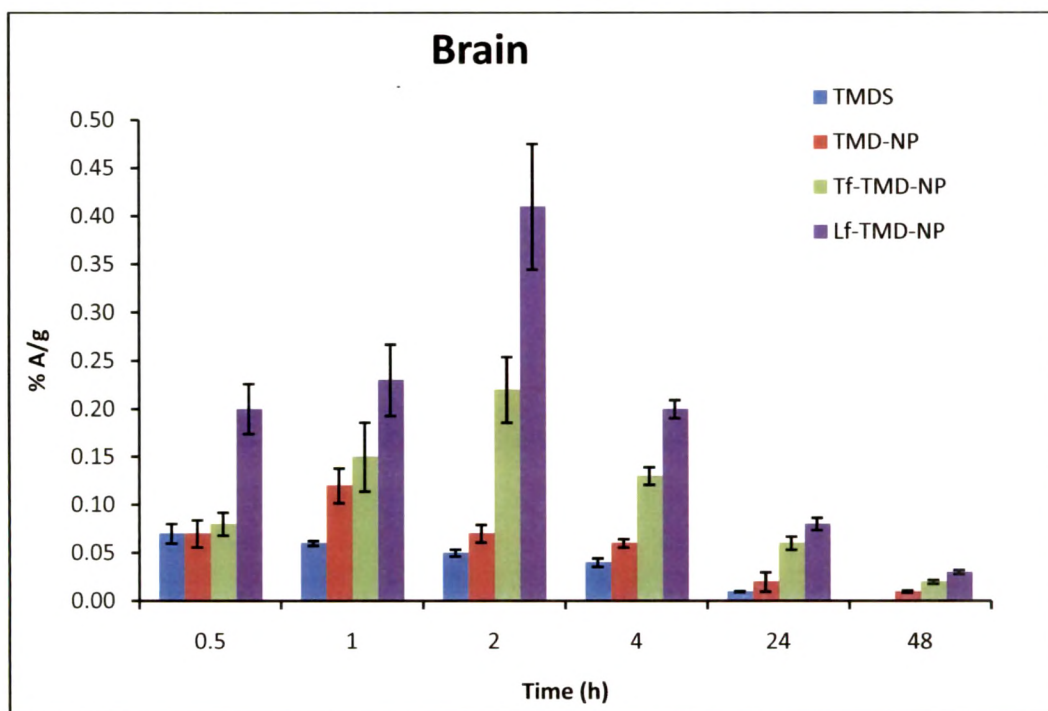


Figure 8.3 Distribution of ^{99m}Tc labelled TMDS and TMD NPs formulations in (A) Liver (B) Spleen (C) Kidney (D) Heart (E) Lung

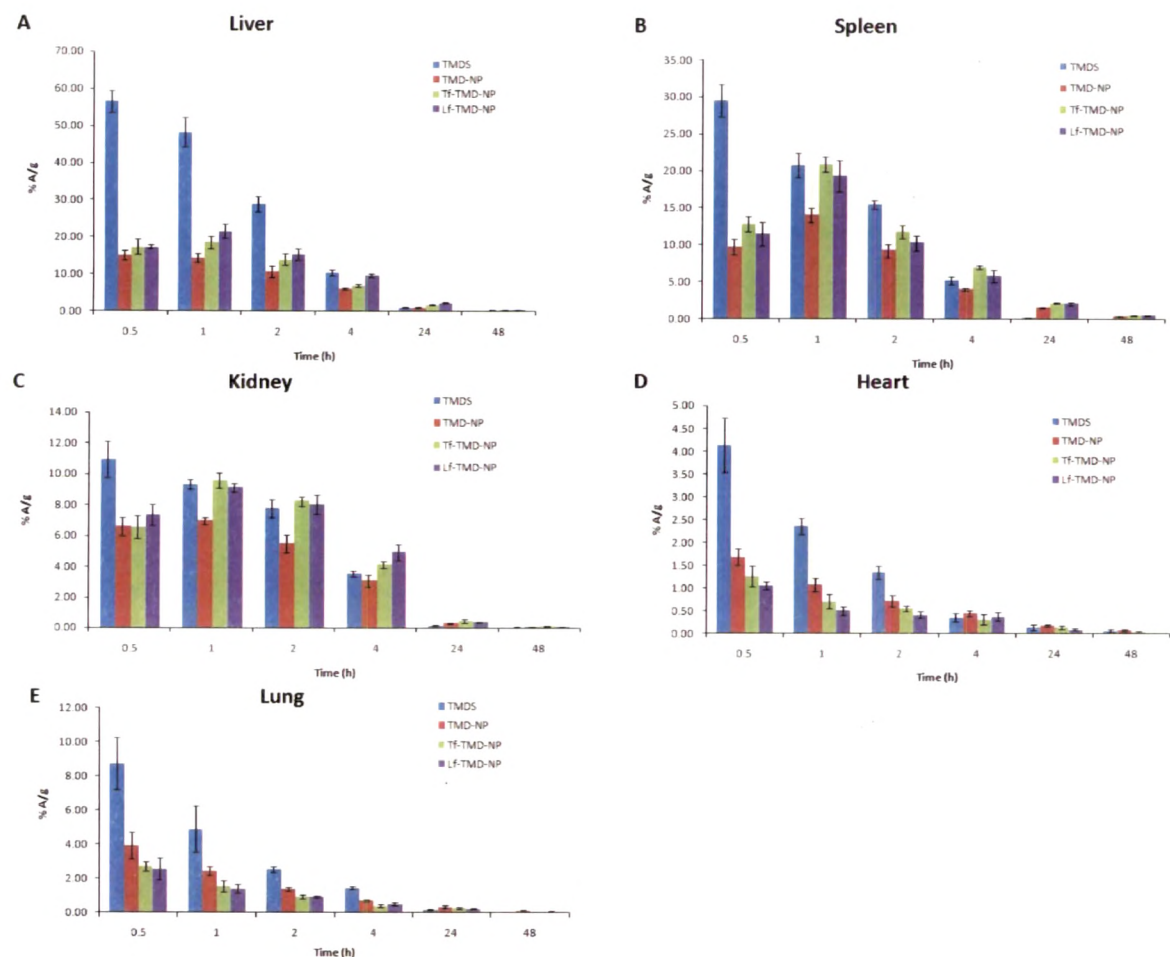


Table 8.5: Pharmacokinetic parameters of blood for TMDS and TMD NPs formulations

Parameter	Formulation			
	TMDS	TMD-NPs	Tf-TMD-NPs	Lf-TMD-NPs
C _{max} (%A/g)	7.16 ± 0.40	7.29 ± 0.24	7.38 ± 0.19	7.21 ± 0.24
T _{max} (h)	0.17	0.17	0.17	0.17
AUC (%A/g h)	25.31 ± 1.03	56.10 ± 3.41*	55.01 ± 0.90*	51.14 ± 2.17*
T _{1/2} (h)	5.67 ± 0.22	15.78 ± 0.63*	14.32 ± 0.39*	13.18 ± 0.38*
MRT (h)	5.06 ± 0.28	18.32 ± 0.83*	16.33 ± 0.55*	14.81 ± 0.71*
Cl (mL/h)	3.79 ± 0.14	1.59 ± 0.09*	1.67 ± 0.03*	1.82 ± 0.13*

Values are represented as mean ± SD, n=3; *significantly different from TMDS, P<0.05

Table 8.6: Pharmacokinetic parameters of brain for TMDS and TMD NPs formulations

Parameter	Formulation			
	TMDS	TMD-NPs	Tf-TMD-NPs	Lf-TMD-NPs
C _{max} (%A/g)	0.07 ± 0.01	0.12 ± 0.02	0.22 ± 0.03*	0.41 ± 0.07* [#]
T _{max} (h)	0.5	1.0	2	2
AUC (%A/g h)	0.59 ± 0.04	1.49 ± 0.11	3.48 ± 0.16*	5.24 ± 0.24* [#]
T _{1/2} (h)	6.72 ± 0.60	12.01 ± 0.61	15.56 ± 0.95*	16.76 ± 0.18*
MRT	7.01 ± 0.80	15.13 ± 0.94	20.65 ± 1.20*	21.22 ± 0.64*

Values are represented as mean ± SD, n=3; *Significantly different from TMDS and TMD-NPs, P<0.05;

[#]Significantly different from Tf-TMD-NPs, P<0.05

Table 8.7: Relative Targeting Ratio of TMD formulations

Comparison mode	Formulations	Ratio value
Targeting with respect to drug solution	TMD-NPs / TMDS	1.14
	Tf-TMD-NPs / TMDS	2.72
	Lf-TMD-NPs / TMDS	4.40
Targeting with respect to plain NPs	Tf-TMD-NPs / TMD-NPs	2.38
	Lf-TMD-NPs / TMD-NPs	3.85
Lf Conjugated NPs with respect to Tf conjugated NPs	Lf-TMD-NPs / Tf-TMD-NPs	1.62

Table 8.8: AUC_(0→48) values of different organs for TMDS and TMD NPs formulations

Organ	Formulation			
	TMDS	TMD-NPs	Tf-TMD-NPs	Lf-TMD-NPs
Liver	248.01 ± 10.65	127.71 ± 7.51	164.55 ± 4.64	209.87 ± 12.22
Spleen	116.39 ± 5.25	111.10 ± 5.27	169.38 ± 6.93	149.20 ± 2.39
Kidney	66.85 ± 2.70	57.61.8 ± 5.77	79.51 ± 5.57	86.15 ± 5.36
Lungs	32.02 ± 1.68	22.87 ± 2.05	14.92 ± 1.99	15.80 ± 1.02
Heart	13.78 ± 0.65	12.85 ± 1.22	9.15 ± 0.85	6.49 ± 0.73
Stomach	0.24 ± 0.02	--	--	--
Intestine	0.31 ± 0.04	--	--	--

Values are represented as mean ± SD, n=3.

Table 8.9: Tissue / Organ distribution of ^{99m}Tc labelled LTGS

Organ/ Tissue	%A/g					
	0.5h	1h	2h	4h	24h	48h
Blood*	5.66 ± 0.15	4.18 ± 0.18	2.45 ± 0.13	1.27 ± 0.07	0.43 ± 0.03	0.09 ± 0.01
Brain	0.24 ± 0.03	0.14 ± 0.01	0.09 ± 0.01	0.05 ± 0.002	0.01 ± 0.001	ND
Liver	39.67 ± 1.78	37.52 ± 2.21	25.68 ± 2.05	10.12 ± 0.88	1.39 ± 0.23	0.27 ± 0.04
Spleen	24.34 ± 1.43	19.45 ± 2.00	14.68 ± 0.87	5.26 ± 0.82	0.47 ± 0.02	0.11 ± 0.01
Kidney	12.85 ± 1.16	11.86 ± 1.23	9.37 ± 0.72	6.32 ± 0.46	0.92 ± 0.06	0.20 ± 0.01
Heart	4.51 ± 0.21	3.75 ± 0.34	2.68 ± 0.27	1.03 ± 0.07	0.26 ± 0.01	0.03 ± 0.001
Lungs	8.66 ± 0.67	5.31 ± 0.91	2.07 ± 0.14	0.88 ± 0.06	0.22 ± 0.03	0.02 ± 0.001
Stomach	0.10 ± 0.01	0.07 ± 0.01	0.05 ± 0.001	0.02 ± 0.001	ND	ND
Intestine	0.13 ± 0.01	0.08 ± 0.01	0.05 ± 0.002	0.03 ± 0.001	ND	ND

Values are represented as mean ± SD, n=3; *0.17h time point for blood was not tabulated

Table 8.10: Tissue / Organ distribution of ^{99m}Tc labelled LTG-NPs

Organ/ Tissue	%A/g					
	0.5h	1h	2h	4h	24h	48h
Blood*	6.58 ± 0.29	4.98 ± 0.39	3.68 ± 0.35	2.11 ± 0.19	0.78 ± 0.06	0.39 ± 0.03
Brain	0.09 ± 0.01	0.17 ± 0.01	0.11 ± 0.001	0.08 ± 0.004	0.04 ± 0.001	0.01 ± 0.001
Liver	11.29 ± 1.33	10.43 ± 1.62	8.77 ± 0.84	6.42 ± 0.26	1.43 ± 0.11	0.34 ± 0.02
Spleen	7.21 ± 0.71	10.43 ± 0.85	8.38 ± 0.69	4.15 ± 0.32	1.83 ± 0.03	0.44 ± 0.03
Kidney	7.12 ± 0.68	6.34 ± 0.39	5.45 ± 0.42	3.62 ± 0.34	0.73 ± 0.05	0.18 ± 0.02
Heart	3.45 ± 0.38	2.17 ± 0.15	1.04 ± 0.15	0.87 ± 0.07	0.14 ± 0.01	0.02 ± 0.001
Lungs	5.21 ± 0.36	2.39 ± 0.17	1.25 ± 0.09	0.81 ± 0.10	0.27 ± 0.02	0.03 ± 0.001

Values are represented as mean ± SD, n=3; *0.17h time point for blood was not tabulated

Table 8.11: Tissue / Organ distribution of ^{99m}Tc labelled Tf-LTG-NPs

Organ/ Tissue	% A/g					
	0.5h	1h	2h	4h	24h	48h
Blood*	6.05 \pm 0.24	4.79 \pm 0.23	3.72 \pm 0.11	2.08 \pm 0.12	0.75 \pm 0.04	0.33 \pm 0.02
Brain	0.13 \pm 0.01	0.26 \pm 0.01	0.24 \pm 0.01	0.15 \pm 0.01	0.08 \pm 0.002	0.03 \pm 0.001
Liver	12.56 \pm 0.76	11.79 \pm 1.18	9.93 \pm 0.53	7.25 \pm 0.61	1.94 \pm 0.15	0.41 \pm 0.04
Spleen	10.42 \pm 1.33	13.21 \pm 1.05	9.45 \pm 0.52	6.82 \pm 0.61	2.42 \pm 0.29	0.72 \pm 0.04
Kidney	8.10 \pm 0.45	7.93 \pm 0.52	6.04 \pm 0.65	4.15 \pm 0.24	1.04 \pm 0.06	0.23 \pm 0.01
Heart	3.10 \pm 0.24	2.03 \pm 0.27	0.91 \pm 0.08	0.62 \pm 0.09	0.11 \pm 0.01	0.02 \pm 0.001
Lungs	2.97 \pm 0.19	1.65 \pm 0.21	0.83 \pm 0.05	0.61 \pm 0.07	0.16 \pm 0.01	0.02 \pm 0.001

Values are represented as mean \pm SD, n=3; *0.17h time point for blood was not tabulated

Table 8.12: Tissue / Organ distribution of ^{99m}Tc labelled Lf-LTG-NPs

Organ/ Tissue	% A/g					
	0.5h	1h	2h	4h	24h	48h
Blood*	5.83 \pm 0.42	4.50 \pm 0.13	3.68 \pm 0.38	1.84 \pm 0.11	0.70 \pm 0.02	0.27 \pm 0.02
Brain	0.17 \pm 0.02	0.29 \pm 0.01	0.26 \pm 0.01	0.21 \pm 0.01	0.13 \pm 0.01	0.04 \pm 0.002
Liver	13.42 \pm 1.41	12.15 \pm 0.95	10.61 \pm 1.17	8.78 \pm 0.69	2.65 \pm 0.23	0.52 \pm 0.04
Spleen	9.45 \pm 0.71	11.89 \pm 1.28	8.67 \pm 1.02	6.13 \pm 0.05	2.28 \pm 0.03	0.61 \pm 0.04
Kidney	8.23 \pm 1.02	8.14 \pm 0.59	6.54 \pm 0.42	4.96 \pm 0.32	1.23 \pm 0.14	0.28 \pm 0.04
Heart	2.05 \pm 0.18	1.70 \pm 0.19	0.64 \pm 0.04	0.41 \pm 0.02	0.07 \pm 0.01	0.01 \pm 0.001
Lungs	3.01 \pm 0.28	1.63 \pm 0.21	0.85 \pm 0.07	0.60 \pm 0.08	0.17 \pm 0.02	0.02 \pm 0.001

Values are represented as mean \pm SD, n=3; *0.17h time point for blood was not tabulated

Figure 8.4 Pharmacokinetic profiles of ^{99m}Tc labelled LTGS and LTG NPs formulations in blood

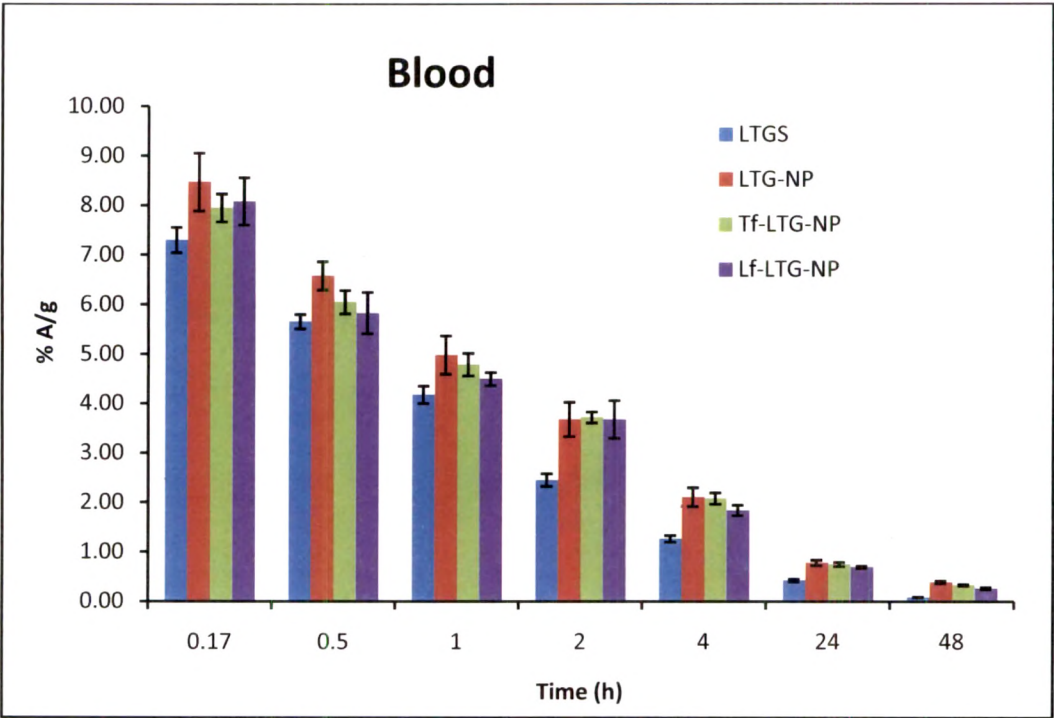


Figure 8.5 Distribution of ^{99m}Tc labelled LTGS and LTG NPs formulations in brain

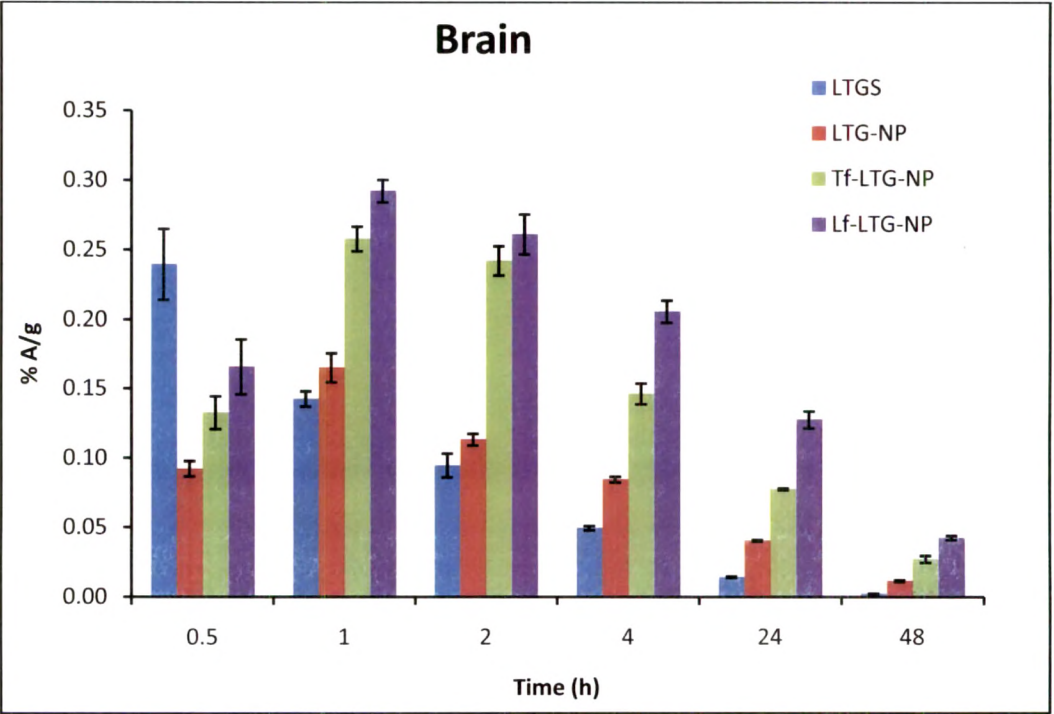


Figure 8.6 Distribution of ^{99m}Tc labelled LTGS and LTG NPs formulations in (A) Liver (B) Spleen (C) Kidney (D) Heart (E) Lung

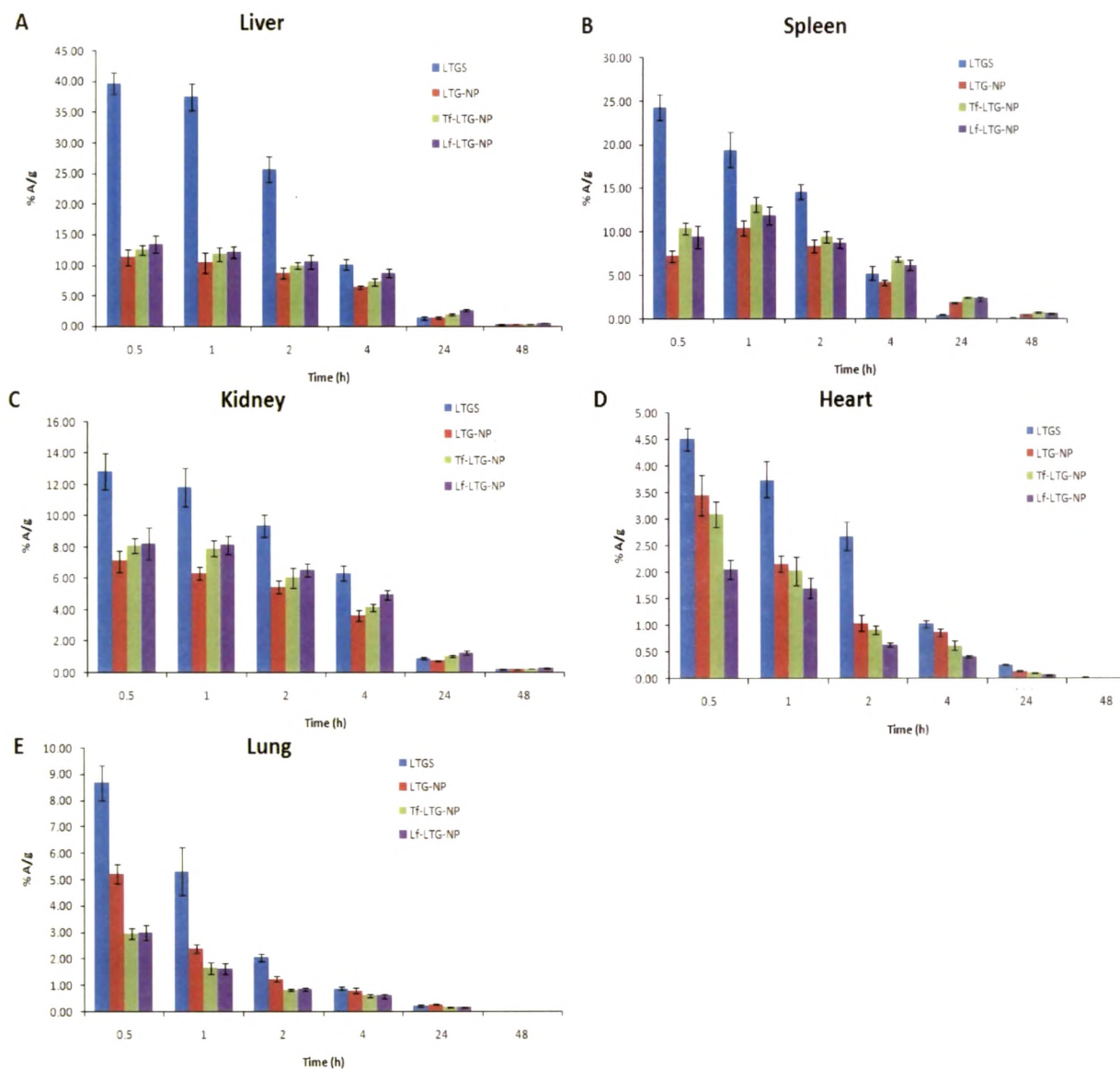


Table 8.13: Pharmacokinetic parameters of blood for LTGS and LTG NPs formulations

Parameter	Formulation			
	TMDS	LTG-NPs	Tf-LTG-NPs	Lf-LTG-NPs
C _{max} (%A/g)	7.30 ± 0.25	8.47 ± 0.58	7.95 ± 0.28	8.08 ± 0.48
T _{max} (h)	0.17	0.17	0.17	0.17
AUC (%A/g h)	36.03 ± 0.44	59.48 ± 1.02*	57.83 ± 1.56*	52.81 ± 2.09*
T _{1/2} (h)	11.34 ± 0.48	18.82 ± 0.58*	16.80 ± 0.40*	15.83 ± 0.62*
MRT (h)	11.60 ± 0.60	22.27 ± 0.89*	19.50 ± 0.48*	17.83 ± 0.86*
Cl (mL/h)	2.67 ± 0.04	1.42 ± 0.03*	1.51 ± 0.03*	1.70 ± 0.07*

Values are represented as mean ± SD, n=3; *Significantly different from LTGS, P<0.05

Table 8.14: Pharmacokinetic parameters of brain for LTGS and LTG NPs formulations

Parameter	Formulation			
	LTGS	LTG-NPs	Tf-LTG-NPs	Lf-LTG-NPs
C _{max} (%A/g)	0.24 ± 0.03	0.17 ± 0.01	0.26 ± 0.01*	0.29 ± 0.01*
T _{max} (h)	0.5	1.0	1.0	1.0
AUC (%A/g h)	1.26 ± 0.01	2.34 ± 0.03	4.32 ± 0.11*	6.37 ± 0.18* [#]
T _{1/2} (h)	10.09 ± 0.06	15.01 ± 0.54	18.10 ± 0.80*	18.60 ± 0.39*
MRT	10.67 ± 0.22	19.31 ± 0.41	23.26 ± 1.11*	25.51 ± 0.59*

Values are represented as mean ± SD, n=3; *Significantly different from LTGS and LTG-NPs, P<0.05;

[#]Significantly different from Tf-LTG-NPs, P<0.05

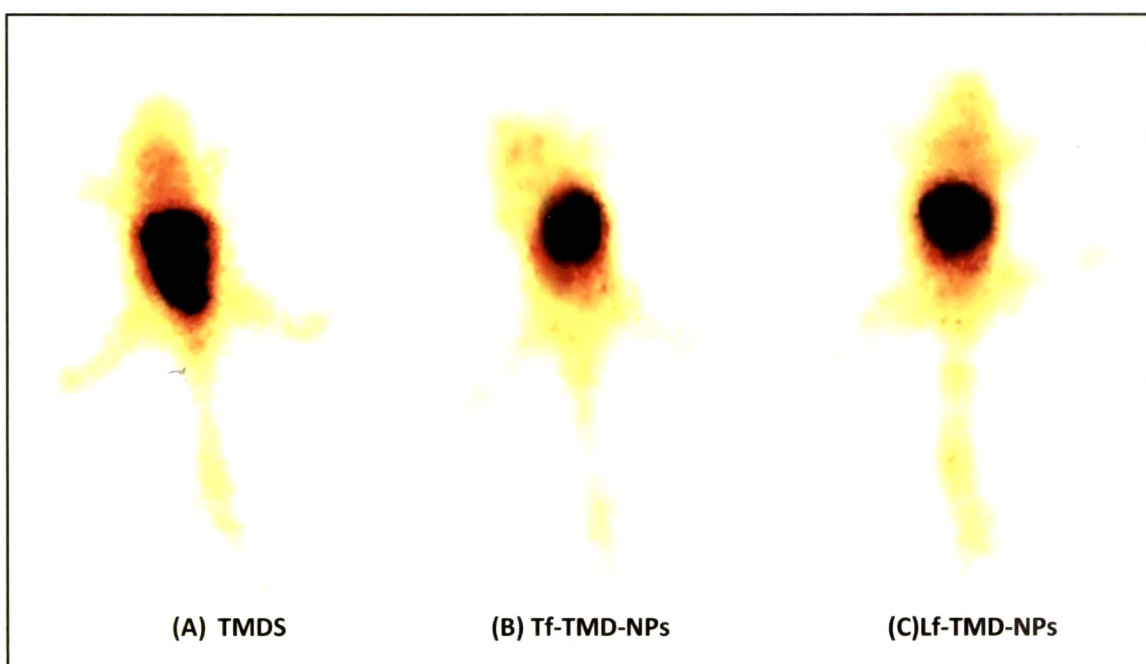
Table 8.15: Relative Targeting Ratio of LTG formulations

Comparison mode	Formulations	Ratio value
Targeting with respect to drug solution	LTG-NPs / LTGS	1.12
	Tf-LTG-NPs / LTGS	2.14
	Lf-LTG-NPs / LTGS	3.45
Targeting with respect to plain NPs	Tf-LTG-NPs / LTG-NPs	1.90
	Lf-LTG-NPs / LTG-NPs	3.07
Lf Conjugated NPs with respect to Tf conjugated NPs	Lf-LTG-NPs / Tf-LTG-NPs	1.61

Table 8.16: $AUC_{(0 \rightarrow 48)}$ values of different organs for LTGS and LTG NPs formulations

Organ	Formulation			
	LTGS	LTG-NPs	Tf-LTG-NPs	Lf-LTG-NPs
Liver	231.72 ± 13.45	132.83 ± 6.48	157.33 ± 7.11	193.93 ± 8.34
Spleen	118.39 ± 7.65	115.16 ± 8.11	166.10 ± 8.59	151.63 ± 4.15
Kidney	121.58 ± 4.78	74.50 ± 5.34	90.48 ± 5.28	104.97 ± 6.21
Lungs	26.18 ± 1.31	21.42 ± 2.02	14.38 ± 1.37	14.49 ± 1.21
Heart	26.50 ± 3.12	17.87 ± 1.02	13.92 ± 0.96	9.38 ± 0.65
Stomach	0.34 ± 0.05	--	--	--
Intestine	0.44 ± 0.02	--	--	--

Values are represented as mean \pm SD, $n=3$.

Figure 8.7 Gamma Scintigraphy image of mice after 2 h of iv administration of (A) TMDS (B) Tf-TMD-NPs (C) Lf-TMD-NPs.

The results of biodistribution for various radiolabeled formulations of TMD in different organs are shown in Table 8.1, 8.2, 8.3, 8.4 and Fig. 8.3. The %A/g versus time profile of TMDS and NPs in blood and brain, obtained after intravenous administration in mice is shown in Fig. 8.1 and 8.2 respectively while, pharmacokinetic parameters are recorded in Table 8.5 and 8.6 respectively. The results of biodistribution for various radiolabelled

formulations of LTG in different organs are shown in Table 8.9, 8.10, 8.11, 8.12 and Figure 8.6. The %A/g versus time profile of LTGS and NPs in blood and brain, obtained after intravenous administration in mice is shown in Fig. 8.4 and 8.5 respectively while, pharmacokinetic parameters are recorded in Table 8.13 and 8.14 respectively.

As observed from Fig. 8.1 and 8.4, concentration of TMDS, LTGS and NPs in blood declined rapidly after intravenous administration. TMD and LTG blood circulation time gets significantly enhanced after its incorporation in PLGA NPs. The plasma AUC_(0→∞), Mean Residence Time (MRT), and $T_{1/2}$ values shown by respective NPs are similar and significantly higher than TMD and LTG. The $T_{1/2}$ and MRT of TMD after incorporation in NPs improves more than two folds. Also, clearance (Cl) of NPs was significantly lesser than TMDS. Similarly, $T_{1/2}$ and MRT of LTG after incorporation in NPs improves by around 1.5 and 1.6 folds respectively. Also, clearance (Cl) of NPs was significantly lesser than LTGS.

The finding shows extended residence time and lower blood clearance of drug from NPs. Better pharmacokinetic profile of NPs may be attributed to slow opsonisation from blood due to smaller size of NPs (<200 nm) (Moghimi SM et al., 1993) and presence of PVA on the NPs surface providing hydrophilic covering around the particles. (Sahoo SK and Labhasetwar V, 2005). Nano-sized PLGA NPs have easy accessibility in the body and transported to different parts of body via systemic circulation, while hydrophilic surface of PVA provide prolonged circulation time for tissue distribution. The internalisation of unconjugated NPs occurs probably by non-specific process.

The distribution of drug in brain is key focus of the present study. Fig. 8.2 shows the brain distribution of TMDS, TMD-NPs, Tf-TMD-NPs and Lf-TMD-NPs. Fig. 8.5 shows the brain distribution of LTGS, LTG-NPs, Tf-LTG-NPs and Lf-LTG-NPs. It is evident from figures that the conjugated and unconjugated NPs demonstrated higher brain deposition than TMDS and LTGS. The overall brain uptake demonstrated by AUC_(0→48) for TMD and LTG formulations are recorded in Table 8.6 and 8.14. The AUC_(0→48) brain for Tf-TMD-NPs and Lf-TMD-NPs was found to be 5.90 folds and 8.88 folds higher than TMDS after intravenous administration. Similarly, The AUC_(0→48) brain for Tf-LTG-NPs and Lf-LTG-NPs were found to be 3.43 folds and 5.05 folds higher than LTGS after intravenous administration.

Higher brain concentrations of NPs can be attributed to prolonged systemic circulation and superior brain transport. $T_{1/2}$ and MRT, indicative parameters for the retention of the drug delivery system in the brain revealed more than 2 folds higher values for conjugated TMD

NPs against TMDS. Similarly, $T_{1/2}$ and MRT of conjugated LTG NPs in the brain revealed more than 1.8 folds higher values than LTGS.

The $AUC_{(0 \rightarrow 48)} \text{ brain} / AUC_{(0 \rightarrow 48)} \text{ blood}$ for TMDS, TMD-NPs, Tf-TMD-NPs and Lf-TMD-NPs were found to be 0.0233, 0.0266, 0.0633 and 0.1025 respectively. The relative targeting ratio for TMDS and different NPs are recorded in Table 8.7. TMD-NPs show marginally higher targeting than TMDS. Tf-TMD-NPs and Lf-TMD-NPs were found to have 2.72 and 4.40 folds higher brain targeting than TMDS and, 2.38 and 3.85 folds higher brain targeting than TMD-NPs. Thus, Tf and Lf ligand conjugation confer preferential uptake by brain endothelial cells and suggest enhanced brain transport. Moreover targeting achieved with Lf conjugation was 1.62 folds higher than Tf conjugation.

The $AUC_{(0 \rightarrow 48)} \text{ brain} / AUC_{(0 \rightarrow 48)} \text{ blood}$ for LTGS, LTG-NPs, Tf-LTG-NPs and Lf-LTG-NPs were found to be 0.0350, 0.0393, 0.0747 and 0.1206 respectively. The relative targeting ratio for LTGS and different NPs are recorded in Table 8.15. LTG-NPs show marginally higher targeting than LTGS. Tf-LTG-NPs and Lf-LTG-NPs were found to have 2.14 and 3.45 folds higher brain targeting than LTGS and, 1.90 and 3.07 folds higher brain targeting than LTG-NPs. Thus, Tf and Lf ligand conjugation confer preferential uptake by brain endothelial cells and suggest enhanced brain transport. Moreover targeting achieved with Lf conjugation was 1.61 folds higher than Tf conjugation.

The Tf and Lf conjugated NPs could have gained an access across the BBB through receptor mediated endocytosis/transcytosis on the membrane (Broadwell RD et al., 1996) The superior uptake of Lf conjugated NPs against Tf conjugated NPs could be primarily because of low circulating concentration of endogenous Lf, approximately 5 nM (Talukder MJ et al., 2003) against higher K_d for brain affinity, thereby avoiding the competitive uptake of endogenous Lf to Lf-conjugated NPs. The membrane preparations of mice brain have high affinity binding site with K_d of about 10.61 nM and the low affinity binding site is with a K_d of about 2228 nM (Huang RQ et al., 2007).

Second, the relatively cationic nature of Lf imparts higher affinity towards the negatively charged cellular membranes. Third, Lf exhibit unidirectional transport across the BBB from the apical to the basolateral side, which leads to higher accumulation of Lf-conjugated drug delivery system formulation in the neuron, compared to Tf counterpart. (Changa J et al., 2009; Broadwell RD et al., 1996) It was demonstrated that Lf receptors exhibited at least two classes of binding sites, with high or low affinity to Lf, in the BBB and brain tissues (Huang RQ et al., 2010). One of the published report showed that exogenous gene expression of Lf-

modified NPs in brains was about 2.3 folds higher than that of Tf-modified NPs (Huang RQ et al., 2008).

The major amount of injected dose was distributed to organs of the RES, such as liver, spleen, and lung. The $AUC_{(0 \rightarrow 48)}$ values of different organs for TMD and LTG formulations are shown in Table 8.8 and 8.16 respectively. TMDS, LTGS and NPs exhibited significant hepatic and splenic uptake. The hepatic accumulations ascertained by $AUC_{(0 \rightarrow 48)}$ indicate 1.51 and 1.18 folds higher deposition for TMDS than Tf-TMD-NPs and Lf-TMD-NPs respectively. Similarly, the hepatic accumulations of LTGS demonstrated 1.47 and 1.19 folds higher deposition than Tf-LTG-NPs and Lf-LTG-NPs respectively.

In liver, the major reason for distribution could be opsonisation and filtration barrier formed by splenic and hepatic cord. Small sterically stabilized particles can distribute mainly to the parenchymal cells of the liver after intravenous administration. (Stolnik S et al., 2001). The low accumulation of unconjugated NPs (TMD-NPs and LTG-NPs) compared to drug solution (TMDS and LTGS) may be due to the hydrophilicity associated with the surface of NPs, as mentioned earlier (Litzinger DC et al., 1994) and higher accumulation of ligand conjugated NPs against unconjugated NPs could be because of presence of Tf (Kawabata H et al., 2001) and Lf receptors in liver (Fillebeen C et al., 1999).

The $AUC_{(0 \rightarrow 48)}$ as shown in Table 8.8 and Table 8.16 displayed significant splenic uptakes of TMDS, LTGS and NPs, however Lf and Tf conjugated NPs revealed higher spleen deposition than their respective drug solutions. The Tf conjugated NPs displayed slightly higher accumulation than their Lf counterpart possibly because of modest presence of LfR against TfR. The phagocytes present in the red pulp of spleen engulf and remove the NPs from systemic circulation. (Litzinger DC et al., 1994) The radioactivity measured indicates higher accumulation of TMDS and LTGS in the lungs than NPs formulation. The conjugated NPs of TMD and LTG shows approx. 1.7 folds lower $AUC_{(0 \rightarrow 48)}$ values (Table 8.8) than TMDS and LTGS respectively for lung. Also the values of radioactivity distribution in heart indicate significantly higher values for TMDS and LTGS than the NPs at all time points. In case of kidney, conjugated NPs demonstrated relatively higher deposition than unconjugated NPs and drug solutions. The moderately higher uptake of conjugated NPs was in agreement with higher uptake observed for Lf distribution in mouse (Huang RQ et al., 2007).

Receptor-mediated endocytosis/transcytosis was considered as the main mechanism of uptake of Lf by organs/cells. The biodistribution data of Tf conjugated NPs are in agreement with the earlier published reports that that mouse TfR are expressed in liver, spleen and kidney

(Kawabata H et al., 2001; Fleming RE et al., 2000). Similarly LfR has been identified in many tissues, including monocytes, lymphocytes and liver (Suzuki YA and Lonnerdal B, 2002). In addition, preferential uptake of Lf by liver paranchymal cells is well reported (Ziere GJ et al., 1992; Debanne MT et al., 1985). The expression of LfR in lymphocyte, monocytes and liver is in accordance with the high accumulation of Lf conjugated NPs in spleen and liver observed in the present study.

To ascertain the organ deposition following intravenous administration of TMDS and ^{99m}TC TMD loaded NPs, gamma scintigraphy was performed and scintigrams after 2 h post intravenous injection are shown in Fig. 8.7. The major radioactivity deposition was seen in liver and spleen for all TMD formulations, in confirmation to the Tissue /Organ distribution studies.

8.3.2 Pharmacokinetics and Biodistribution studies of Microemulsion and Nanoemulsion

The radiolabeled complexes of TS_{in} , TME and TNE were evaluated for biodistribution in healthy swiss mice for 24 h after intravenous administration. The results of biodistribution for various radiolabelled complexed formulations are tabulated in Table 8.17, 8.18 and 8.19. The radiolabeled complexes of LS_{in} , LME and LNE were evaluated for biodistribution in healthy swiss mice for 48 h after intravenous administration. The results of biodistribution for various radiolabelled complexed formulations are tabulated in Table 8.23, 8.24 and 8.25.

Table 8.17: Tissue / Organ distribution of ^{99m}TC labelled TS_{in}

Organ/ Tissue	%A/g					
	0.5h	1h	2h	4h	8h	24h
Blood*	0.12 ± 0.02	0.23 ± 0.04	0.16 ± 0.02	0.11 ± 0.001	0.05 ± 0.002	0.01 ± 0.001
Brain	0.07 ± 0.01	0.05 ± 0.001	0.04 ± 0.001	0.03 ± 0.001	0.02 ± 0.001	ND
Liver	0.61 ± 0.05	0.78 ± 0.10	0.67 ± 0.06	0.48 ± 0.04	0.17 ± 0.02	0.02 ± 0.001
Spleen	0.26 ± 0.03	0.36 ± 0.02	0.32 ± 0.02	0.17 ± 0.01	0.09 ± 0.01	0.01 ± 0.001
Kidney	0.11 ± 0.01	0.17 ± 0.01	0.14 ± 0.02	0.11 ± 0.01	0.09 ± 0.01	0.01 ± 0.001
Lungs	0.14 ± 0.01	0.17 ± 0.02	0.13 ± 0.01	0.09 ± 0.01	0.03 ± 0.001	ND
Stomach	0.31 ± 0.02	0.28 ± 0.03	0.21 ± 0.02	0.13 ± 0.01	0.04 ± 0.001	0.01 ± 0.001
Intestine	0.04 ± 0.01	0.13 ± 0.01	0.20 ± 0.02	0.14 ± 0.01	0.09 ± 0.01	0.01 ± 0.001

Values are represented as mean \pm SD, n=3; *0.17h time point for blood was not tabulated

Table 8.18: Tissue / Organ distribution of ^{99m}Tc labelled TME

Organ/ Tissue	% A/g					
	0.5h	1h	2h	4h	8h	24h
Blood*	0.13 \pm 0.02	0.26 \pm 0.02	0.17 \pm 0.01	0.12 \pm 0.01	0.07 \pm 0.01	0.01 \pm 0.001
Brain	0.36 \pm 0.02	0.34 \pm 0.03	0.22 \pm 0.02	0.12 \pm 0.01	0.07 \pm 0.001	0.02 \pm 0.001
Liver	0.81 \pm 0.07	1.11 \pm 0.06	0.96 \pm 0.08	0.67 \pm 0.05	0.27 \pm 0.02	0.03 \pm 0.002
Spleen	0.35 \pm 0.04	0.54 \pm 0.03	0.43 \pm 0.05	0.28 \pm 0.02	0.18 \pm 0.01	0.01 \pm 0.001
Kidney	0.19 \pm 0.02	0.27 \pm 0.03	0.20 \pm 0.01	0.14 \pm 0.01	0.10 \pm 0.01	0.01 \pm 0.001
Lungs	0.14 \pm 0.01	0.19 \pm 0.02	0.16 \pm 0.01	0.13 \pm 0.01	0.04 \pm 0.002	0.05 \pm 0.004
Stomach	0.28 \pm 0.03	0.22 \pm 0.02	0.16 \pm 0.01	0.09 \pm 0.01	0.04 \pm 0.001	ND
Intestine	0.02 \pm 0.001	0.09 \pm 0.01	0.16 \pm 0.01	0.09 \pm 0.01	0.05 \pm 0.003	0.01 \pm 0.001

Values are represented as mean \pm SD, n=3. ND-Not Detected; *0.17h time point for blood was not tabulated

Table 8.19: Tissue / Organ distribution of ^{99m}Tc labelled TNE

Organ/ Tissue	% A/g					
	0.5h	1h	2h	4h	8h	24h
Blood*	0.12 \pm 0.01	0.23 \pm 0.02	0.15 \pm 0.02	0.12 \pm 0.01	0.07 \pm 0.01	0.01 \pm 0.001
Brain	0.32 \pm 0.02	0.29 \pm 0.01	0.20 \pm 0.01	0.12 \pm 0.01	0.06 \pm 0.004	0.01 \pm 0.001
Liver	0.73 \pm 0.06	1.01 \pm 0.08	0.88 \pm 0.07	0.59 \pm 0.02	0.22 \pm 0.02	0.03 \pm 0.002
Spleen	0.33 \pm 0.02	0.45 \pm 0.06	0.39 \pm 0.02	0.22 \pm 0.03	0.16 \pm 0.01	0.01 \pm 0.001
Kidney	0.17 \pm 0.02	0.22 \pm 0.01	0.20 \pm 0.02	0.12 \pm 0.01	0.09 \pm 0.01	0.01 \pm 0.001
Lungs	0.13 \pm 0.01	0.19 \pm 0.02	0.14 \pm 0.01	0.12 \pm 0.01	0.04 \pm 0.002	0.01 \pm 0.001
Stomach	0.28 \pm 0.03	0.22 \pm 0.02	0.16 \pm 0.01	0.09 \pm 0.01	0.04 \pm 0.002	ND
Intestine	0.03 \pm 0.002	0.09 \pm 0.01	0.17 \pm 0.02	0.10 \pm 0.01	0.06 \pm 0.003	0.01 \pm 0.001

Values are represented as mean \pm SD, n=3; *0.17h time point for blood was not tabulated

Figure 8.8 Pharmacokinetic profiles of ^{99m}Tc labelled TS, TME and TNE in blood

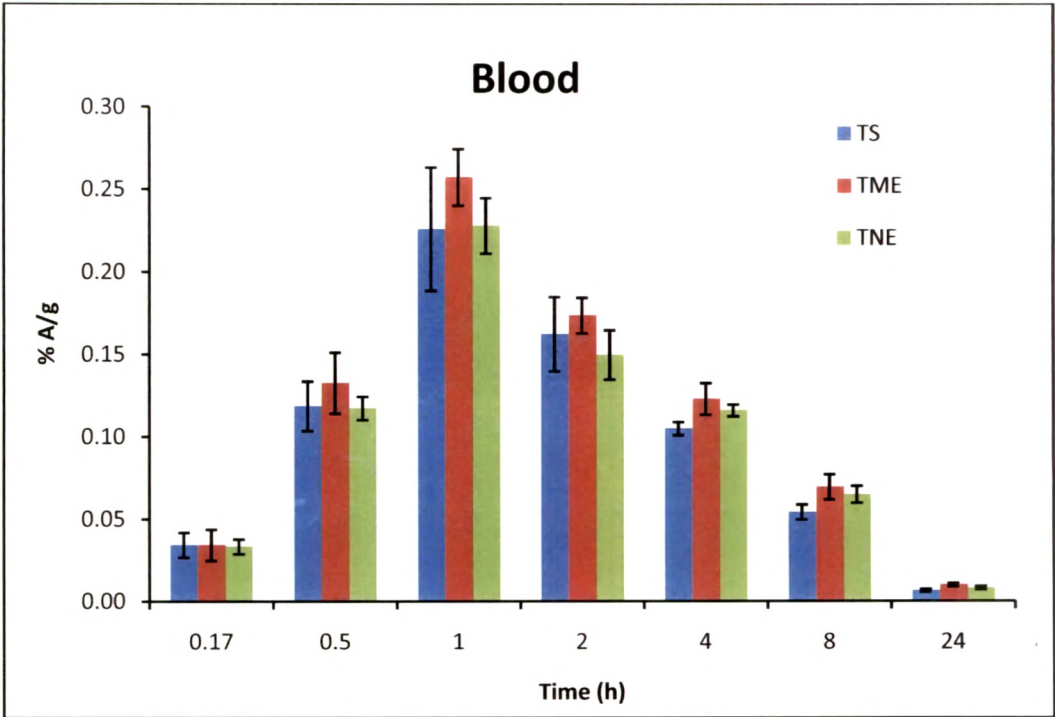


Figure 8.9 Distribution of ^{99m}Tc labelled TS, TME and TNE in brain

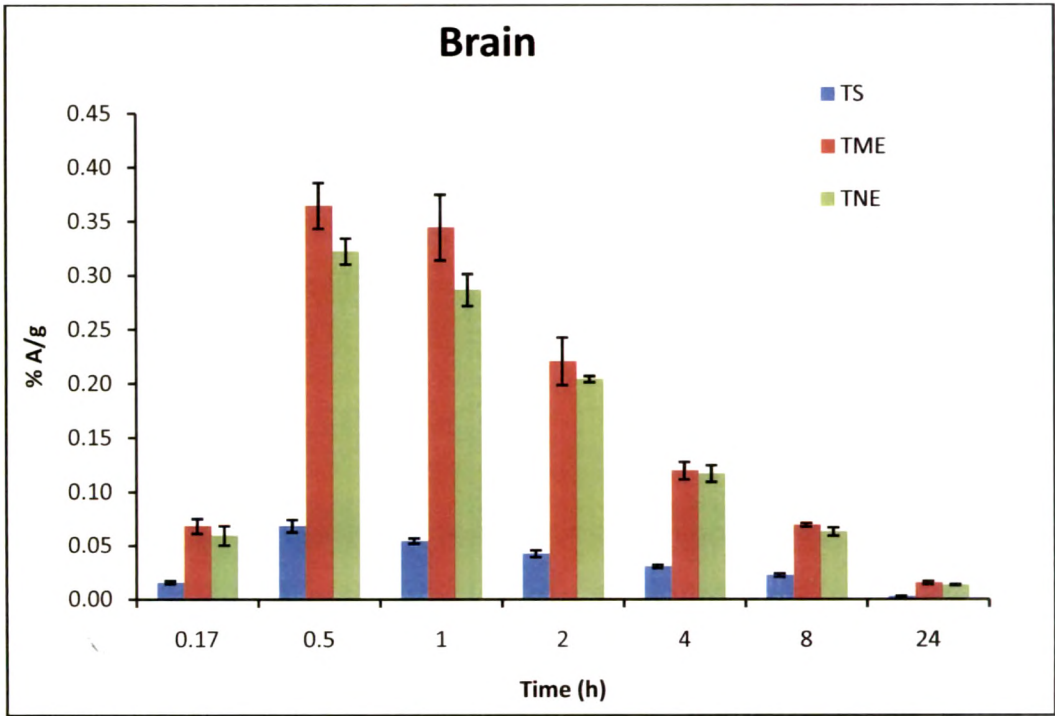


Figure 8.10 Distribution of ^{99m}Tc labelled TS, TME and TNE in (A) Liver (B) Spleen (C) Kidney (D) Lung (E) Stomach (F) Intestine

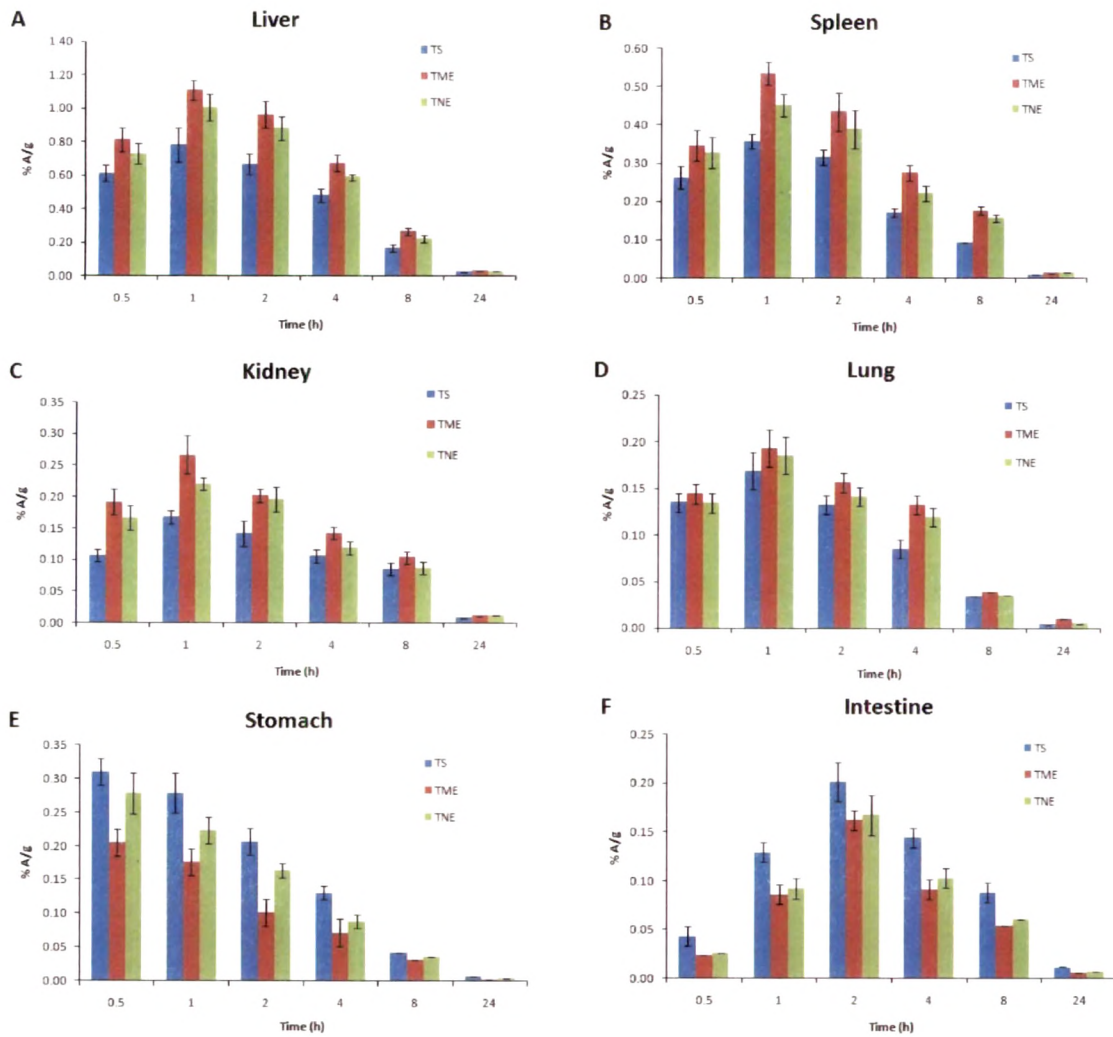


Table 8.20: Pharmacokinetic parameters of blood and brain for TS_{iv}, TS_{in}, TME and TNE

Parameter	Organ	TS _{iv}	TS _{in}	TME	TNE
C _{max} (%A/g)	Blood	7.16 ± 0.40	0.23 ± 0.04	0.26 ± 0.02	0.23 ± 0.02
	Brain	0.07 ± 0.01	0.07 ± 0.01*	0.36 ± 0.02	0.32 ± 0.01*
T _{max} (h)	Blood	0.17	1.0	1.0	1.0
	Brain	0.5	0.5	0.5	0.5
AUC _(0→48) (%A/g h)	Blood	25.10 ± 1.14	1.38 ± 0.07	1.66 ± 0.05*	1.48 ± 0.04
	Brain	0.57 ± 0.02	0.43 ± 0.02	1.90 ± 0.04*	1.73 ± 0.04*
T _{1/2} (h)	Blood	5.64 ± 0.23	5.20 ± 0.28	5.56 ± 0.28	5.46 ± 0.44
	Brain	6.62 ± 0.53	5.57 ± 0.19	6.91 ± 0.22	6.59 ± 0.10
MRT (h)	Blood	6.47 ± 0.30	6.46 ± 0.05	7.04 ± 0.37	7.09 ± 0.51
	Brain	8.58 ± 0.65	8.24 ± 0.14	7.82 ± 0.49	7.57 ± 0.24
% Nasal	Blood	--	5.50	6.61	5.90
bioavailability	Brain	--	74.74	333.33*	303.51*

Values are represented as mean ± SD, n=3; *significantly different from TS_{in}, P<0.05

Table 8.21 Brain targeting efficiency and direct nose to brain transport percentage following i.n. administration of ^{99m}Tc labelled TS_{iv}, TS_{in}, TS, TME and TNE

Formulation	Brain targeting efficiency (DTE (%))	Direct nose to brain transport percentage (DTP (%))
TS _{iv}	2.27	--
TS _{in}	31.16	92.71
TME	114.46*	98.02
TNE	116.89*	98.06

*Significantly different from TS_{iv} and TS_{in}, P<0.05.

Table 8.22: AUC_(0→48) values of different organs for TS_{iv}, TS_{in}, TME, and TNE

Organ	Formulation			
	TS _{iv}	TS _{in}	TME	TNE
Liver	248.42 ± 10.59	5.20 ± 0.61	7.55 ± 0.32	6.69 ± 0.41
Spleen	114.14 ± 5.24	2.33 ± 0.12	3.93 ± 0.41	3.46 ± 0.24
Kidney	65.81 ± 2.66	1.67 ± 0.09	2.12 ± 0.16	1.90 ± 0.13
Lungs	31.19 ± 1.64	1.04 ± 0.11	1.28 ± 0.06	1.16 ± 0.08
Stomach	0.24 ± 0.02	1.57 ± 0.07	0.95 ± 0.08	1.24 ± 0.04
Intestine	0.31 ± 0.04	1.85 ± 0.14	1.20 ± 0.06	1.28 ± 0.10

Values are represented as mean ± SD, n=3.

Table 8.23: Tissue / Organ distribution of ^{99m}Tc labelled LS_{in}

Organ/ Tissue	% A/g						
	0.5h	1h	2h	4h	8h	24h	48h
Blood*	0.12 ± 0.01	0.18 ± 0.02	0.13 ± 0.01	0.11 ± 0.001	0.07 ± 0.01	0.02 ± 0.001	0.01 ± 0.001
Brain	0.18 ± 0.02	0.13 ± 0.01	0.09 ± 0.01	0.05 ± 0.002	0.03 ± 0.001	0.01 ± 0.001	ND
Liver	0.78 ± 0.01	0.86 ± 0.06	0.74 ± 0.09	0.61 ± 0.03	0.39 ± 0.04	0.12 ± 0.01	0.02 ± 0.001
Spleen	0.27 ± 0.02	0.38 ± 0.02	0.23 ± 0.02	0.16 ± 0.01	0.10 ± 0.01	0.02 ± 0.001	ND
Kidney	0.09 ± 0.01	0.15 ± 0.01	0.13 ± 0.01	0.11 ± 0.01	0.08 ± 0.01	0.02 ± 0.001	ND
Lungs	0.13 ± 0.01	0.16 ± 0.02	0.13 ± 0.01	0.09 ± 0.01	0.05 ± 0.003	0.01 ± 0.001	ND
Stomach	0.29 ± 0.02	0.27 ± 0.03	0.21 ± 0.01	0.14 ± 0.01	0.06 ± 0.004	0.01 ± 0.001	ND
Intestine	0.04 ± 0.01	0.11 ± 0.02	0.17 ± 0.01	0.15 ± 0.01	0.10 ± 0.01	0.02 ± 0.001	ND

Values are represented as mean ± SD, n=3. ND-Not Detected; *0.17h time point for blood was not tabulated

Table 8.24: Tissue / Organ distribution of ^{99m}Tc labelled LME

Organ/ Tissue	% A/g						
	0.5h	1h	2h	4h	8h	24h	48h
Blood*	0.14 ± 0.01	0.22 ± 0.03	0.15 ± 0.01	0.13 ± 0.01	0.07 ± 0.01	0.02 ± 0.001	0.01 ± 0.001
Brain	0.32 ± 0.01	0.30 ± 0.01	0.23 ± 0.01	0.16 ± 0.01	0.09 ± 0.01	0.03 ± 0.001	0.01 ± 0.001
Liver	1.27 ± 0.15	1.36 ± 0.09	1.13 ± 0.12	0.96 ± 0.13	0.70 ± 0.02	0.20 ± 0.02	0.03 ± 0.002
Spleen	0.39 ± 0.05	0.58 ± 0.04	0.34 ± 0.02	0.22 ± 0.02	0.15 ± 0.01	0.03 ± 0.002	ND
Kidney	0.17 ± 0.02	0.22 ± 0.01	0.18 ± 0.02	0.14 ± 0.01	0.11 ± 0.01	0.02 ± 0.001	ND
Lungs	0.13 ± 0.01	0.18 ± 0.02	0.14 ± 0.02	0.12 ± 0.01	0.06 ± 0.01	0.01 ± 0.001	ND
Stomach	0.20 ± 0.01	0.17 ± 0.02	0.12 ± 0.02	0.08 ± 0.01	0.03 ± 0.001	0.01 ± 0.001	ND
Intestine	0.02 ± 0.001	0.08 ± 0.01	0.14 ± 0.02	0.10 ± 0.01	0.06 ± 0.01	0.01 ± 0.001	ND

Values are represented as mean ± SD, n=3. ND-Not Detected; *0.17h time point for blood was not tabulated

Table 8.25: Tissue / Organ distribution of ^{99m}Tc labelled LNE

Organ/ Tissue	%A/g						
	0.5h	1h	2h	4h	8h	24h	48h
Blood*	0.14 ± 0.03	0.20 ± 0.02	0.13 ± 0.01	0.12 ± 0.01	0.07 ± 0.004	0.02 ± 0.001	0.01 ± 0.001
Brain	0.27 ± 0.01	0.24 ± 0.01	0.19 ± 0.01	0.14 ± 0.01	0.08 ± 0.01	0.02 ± 0.001	0.01 ± 0.001
Liver	0.98 ± 0.06	1.11 ± 0.07	0.90 ± 0.10	0.78 ± 0.11	0.54 ± 0.02	0.14 ± 0.01	0.02 ± 0.001
Spleen	0.33 ± 0.04	0.44 ± 0.03	0.33 ± 0.02	0.20 ± 0.02	0.12 ± 0.01	0.02 ± 0.001	ND
Kidney	0.14 ± 0.01	0.18 ± 0.02	0.15 ± 0.01	0.13 ± 0.01	0.09 ± 0.01	0.02 ± 0.001	ND
Lungs	0.12 ± 0.01	0.17 ± 0.02	0.13 ± 0.01	0.11 ± 0.01	0.05 ± 0.003	0.01 ± 0.001	ND
Stomach	0.22 ± 0.01	0.20 ± 0.02	0.16 ± 0.01	0.11 ± 0.01	0.05 ± 0.01	0.01 ± 0.001	ND
Intestine	0.02 ± 0.001	0.08 ± 0.01	0.15 ± 0.01	0.10 ± 0.01	0.07 ± 0.003	0.01 ± 0.001	ND

Values are represented as mean \pm SD, n=3. ND-Not Detected; *0.17h time point for blood was not tabulated

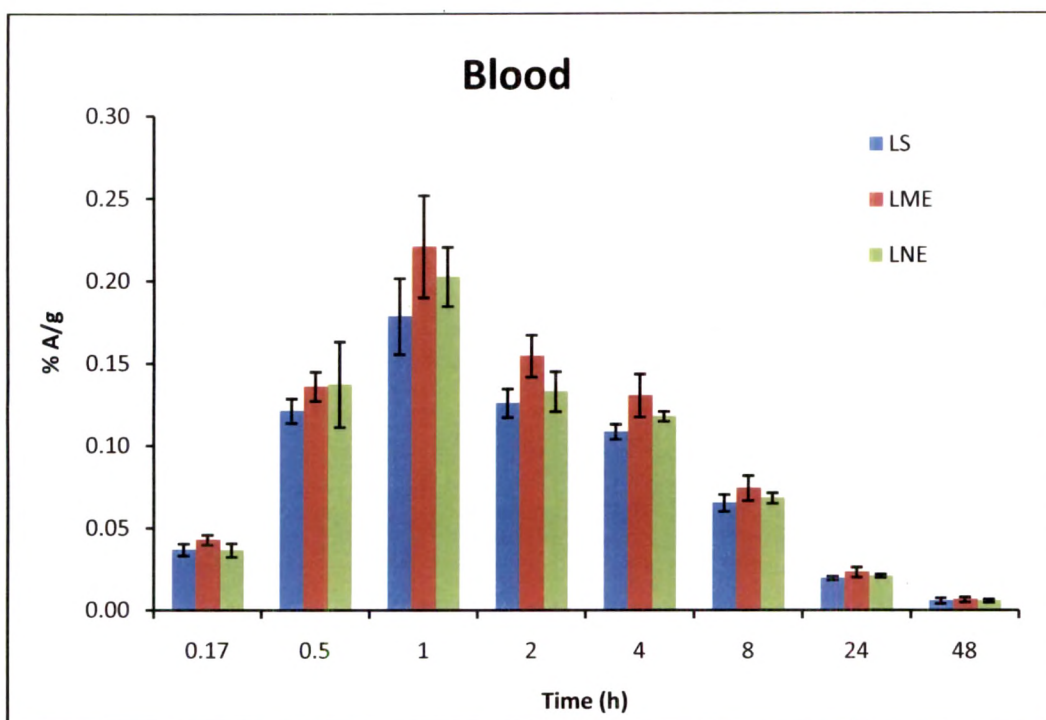
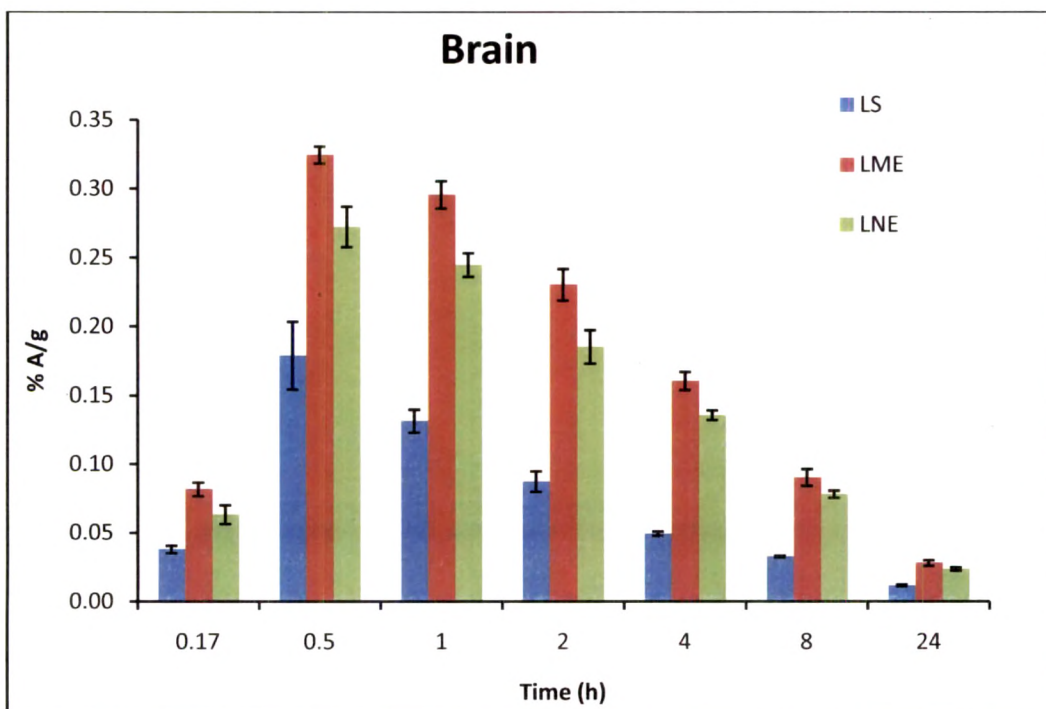
Figure 8.11 Pharmacokinetic profiles of ^{99m}Tc labelled LS, LME and LNE in blood**Figure 8.12** Distribution of ^{99m}Tc labelled LS, LME and LNE in brain

Figure 8.13 Distribution of ^{99m}Tc labelled LS, LME and LNE in various organs (A) Liver (B) Spleen (C) Kidney (D) Lung (E) Stomach (F) Intestine

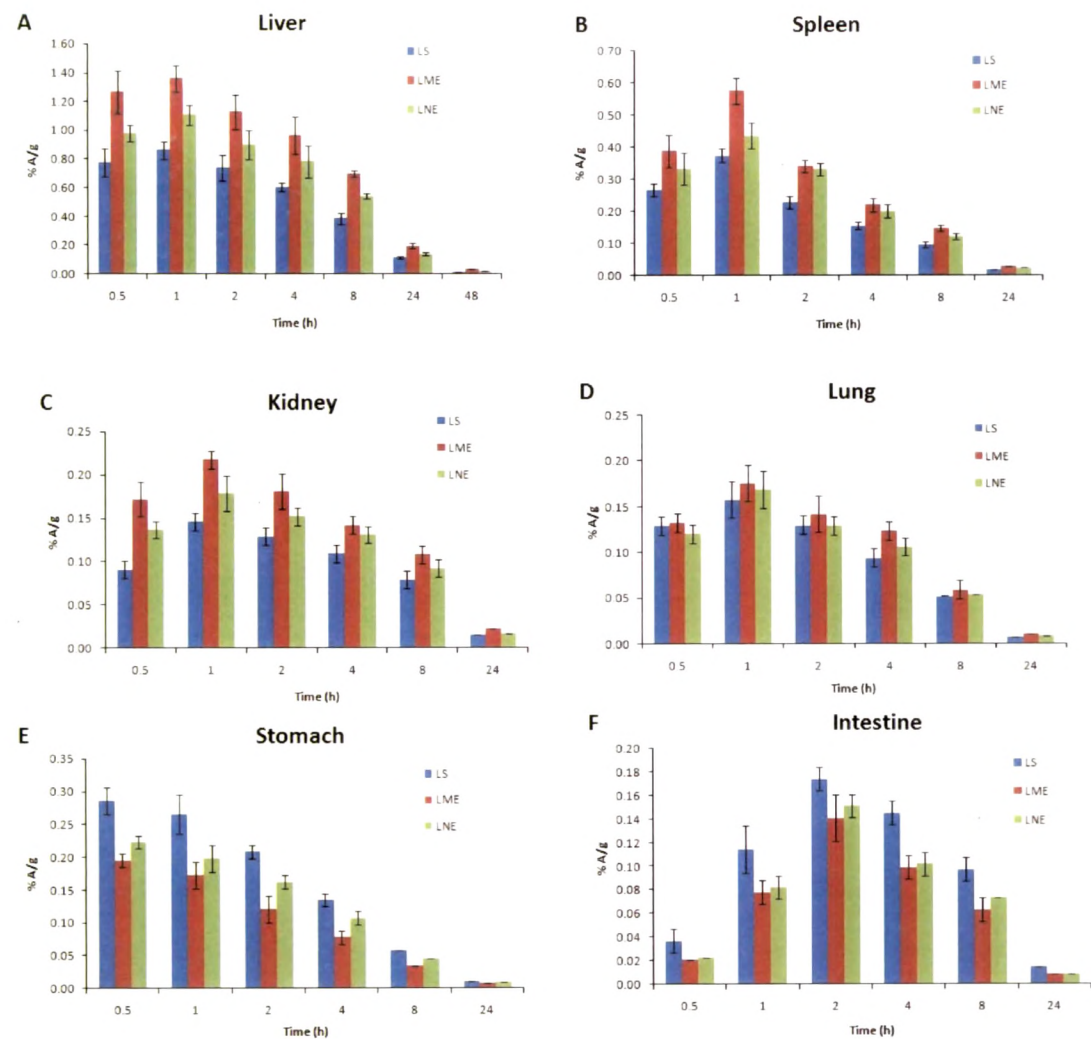


Table 8.26: Pharmacokinetic parameters of blood and brain for LS_{iv}, LS_{in}, LME, and LNE

Parameter	Organ	LS _{iv}	LS _{in}	LME	LNE
C _{max} (%A/g)	Blood	7.30 ± 0.25	0.18 ± 0.02	0.22 ± 0.03	0.20 ± 0.02
	Brain	0.24 ± 0.03	0.18 ± 0.02	0.32 ± 0.01	0.27 ± 0.01
T _{max} (h)	Blood	0.17	1.0	1.0	1.0
	Brain	0.5	0.5	0.5	0.5
AUC _(0→48) (%A/g h)	Blood	36.03 ± 0.44	1.82 ± 0.07	2.14 ± 0.23	1.94 ± 0.08
	Brain	1.23 ± 0.02	1.05 ± 0.02	2.74 ± 0.14*	2.31 ± 0.09*
T _{1/2} (h)	Blood	11.34 ± 0.48	11.02 ± 0.14	11.57 ± 0.66	11.04 ± 0.22
	Brain	9.91 ± 0.23	10.08 ± 0.25	10.04 ± 0.25	10.11 ± 0.65
MRT (h)	Blood	11.60 ± 0.60	13.29 ± 0.77	13.33 ± 0.88	13.28 ± 0.89
	Brain	11.78 ± 0.44	11.48 ± 0.30	11.34 ± 0.30	11.52 ± 0.56
% Nasal	Blood	--	5.05	5.94	5.38
bioavailability	Brain	--	85.37	222.76*	187.80*

Values are represented as mean ± SD, n=3; *Significantly different from LS_{in}, P<0.05

Table 8.27 Brain targeting efficiency and Direct nose to brain transport percentage following i.n. administration of ^{99m}Tc labeled LS_{iv}, LS_{in}, LME and LNE

Formulation	Brain targeting efficiency (DTE (%))	Direct nose to brain transport percentage (DTP (%))
LS _{iv}	3.41	--
LS _{in}	57.96	94.08
LME	128.04*	97.33
LNE	119.07*	97.13

*Significantly different from LS_{iv} and LS_{in}, P<0.05.

Table 8.28: AUC_(0→48) values of different organs for LS_{iv}, LS_{in}, LME and LNE

Organ	Formulation			
	LS _{iv}	LS _{in}	LME	LNE
Liver	230.20 ± 13.19	10.39 ± 0.98	17.57 ± 1.35	13.56 ± 1.08
Spleen	114.81 ± 7.43	2.33 ± 0.15	3.87 ± 0.26	3.36 ± 0.21
Kidney	118.28 ± 4.65	1.89 ± 0.16	2.54 ± 0.29	2.15 ± 0.26
Lungs	26.08 ± 1.28	1.25 ± 0.07	1.48 ± 0.09	1.33 ± 0.12
Stomach	0.35 ± 0.05	1.88 ± 0.14	1.03 ± 0.10	1.34 ± 0.06
Intestine	0.45 ± 0.02	1.91 ± 0.13	1.23 ± 0.06	1.43 ± 0.08

Values are represented as mean ± SD, n=3.

Reports in the literature reveal that the drug uptake into the brain from the nasal mucosa mainly occurs via three different pathways (Illum L, 2003; Vyas TK et al., 2005; Thorne RG et al., 2004). One is the systemic pathway by which some of the drug is absorbed into the systemic circulation and subsequently reaches the brain by crossing BBB. The others are the olfactory pathway and the trigeminal neural pathway by which partly the drug travels directly from the nasal cavity to CSF and brain tissue. We can conclude that the amount of drug reaches in the brain tissue after nasal administration is attributed to these three pathways. Therefore, DTP (%) represents the percentage of drug directly transported to the brain via the olfactory pathway and the trigeminal neural pathway.

The pharmacokinetic parameters C_{max} , T_{max} , $AUC_{(0 \rightarrow 48)}$, half life, MRT and nasal bioavailability were calculated and given in Table 8.20 and 8.26 for TMD and LTG formulations. C_{max} and $AUC_{(0 \rightarrow 48)}$ of blood for TS_{in} are respectively more than 27 and 15 folds lower than TS_{iv} . However, brain concentration for TME and TNE was significantly higher. Similarly, C_{max} and $AUC_{(0 \rightarrow 48)}$ of blood for LS_{in} are respectively more than 33 and 16 folds lower than LS_{iv} . However, brain concentration for LME and LNE was significantly higher. Drug transport from nose to brain, for all i.n formulations, as reflected by DTP values, was contributing more 90%. This is attributed to preferential nose to brain transport following nasal administration. The brain/blood ratios of drug at all time points were found to be higher following i.n. administration of the formulations than i.v. solution. This further confirms direct nose to brain transport (Illum L, 2000; Lianli L et al., 2002).

$AUC_{(0 \rightarrow 48)}$ brain for TME and TNE increased by 2-3 folds as compared to their respective solutions after i.n. administration. The enhancement of AUC in brain followed by i.n. ME and NE are in congruence with the observations reported by Lianli L et al (2002) and Zhang et al. (2004) that microemulsion enhances the transport of drug across nasal mucosa. T_{max} , values observed in brain for solutions, MEs and NEs of TMD and LTG was 0.5 h. It is indicative of rapid transport from nose to brain. Half life and MRT of TS_{in} , TME and TNE for both blood and brain are similar to that of TS_{iv} . Similarly, half life and MRT of LS_{in} , LME and LNE for both blood and brain are similar to that of LS_{iv} .

Targeting efficiency of formulations is reflected by %DTE. As shown in Table 8.21, targeting achieved with TME and TNE was around 3.6 times higher than that of solution and 50 times higher than TS_{iv} . As shown in Table 8.27, targeting of achieved with LME and LNE was around 2 times higher than that of solution and 37 times higher than LS_{iv} . The higher concentration of drug in brain following i.n administration of TME, TNE, LME and LNE

demonstrates the suitability and capability of microemulsion as an effective delivery system across the nasal membrane (Lawrence MJ and Rees GD, 2000) and a larger extent of selective transport of drug from nose to brain. This is in agreement with published reported stating unique connection between the nose and brain and drug transport to brain circumventing the BBB after i.n. administration. (Behl CR et al., 1998; Illum L, 2000) Nasal bioavailability of TME and TNE was 6 folds higher than TS_{iv} while nasal bioavailability of LME and LNE was 2-3 folds higher than LS_{in} . Though ME system for TMD and LTG demonstrated higher targeting efficiency than their respective solution but difference was nonsignificant ($P > 0.05$).

The $AUC_{(0 \rightarrow 48)}$ values of different organs for TMD and LTG formulations are shown in Table 8.22 and 8.28 respectively. Organ distribution data shows that only minor amount of ME and NE goes to liver, spleen, kidney and lungs compared to their respective solution administered intravenously. In case of stomach and kidney, $AUC_{(0 \rightarrow 48)}$ for ME and NE were higher than solution administered intravenously. This may be due to fraction of dose entered GI tract from nasal cavity after i.n. administration.

8.4 Conclusion

TMD & LTG exhibited higher brain uptake after incorporation in PLGA nanoparticles as compared to solution. Nano-sized PLGA nanoparticles have easy accessibility in the body and transported to different parts of body via systemic circulation, while hydrophilic surface of PVA provide prolonged circulation time for tissue distribution. The internalisation of unconjugated nanoparticles occurs probably by non-specific process.

The Tf and Lf conjugated PLGA nanoparticles showed a promising targeted delivery to the brain. Significant improvement in brain uptake was observed following intravenous administration of conjugated nanoparticles compared to unconjugated nanoparticles due to receptor mediated intracellular endocytosis through Tf and Lf receptors present in the blood brain barrier. Functionalization of the NP with Lf was proved to be superior to Tf, for facilitating their translocation into the brain tissue after intravenous administration. Though Tf and Lf exhibit structural similarity and homology, the distribution of their respective receptors being different, it directs the difference in the tissue distribution of Tf and Lf conjugated PLGA nanoparticles. Primarily the low endogenous concentration and additionally, cationic charge and unidirectional transport as observed with Lf are supposed to be the major reason for enhanced uptake of Lf conjugated nanoparticles in brain when

compared against Tf conjugated nanoparticles. The expression of LfR varied among different animals, hence further, more animal studies followed by extensive toxicological evaluation are necessary to confirm the role of Lf conjugated nanoparticles for brain delivery.

Biodistribution studies revealed that intranasal administration of ME and NE of TMD and LTG ensures effective and rapid brain delivery executed by direct nose to brain transport. Higher DTP value confirms role of direct nasal-brain transport while higher DTE confirm role of ME and NE as delivery system for nose to brain transport. Though ME show higher transport but was not significantly different from NE. Direct transport of drugs to the brain may lead to the administration of lower doses, reduce the toxicity and, avoids systemic dilution effect and first pass metabolism.

It would be necessary to consider the anatomical differences between rats and human beings, the olfactory and respiratory epithelia of the rat are interspersed throughout the entire nasal mucosa, while in humans the olfactory epithelium is present only at the roof of the nasal cavity. It seems disadvantageous for the drug transport into CNS via the olfactory pathway when applied in human compared with rodents. To overcome this disadvantage, the retention time of the drug over the olfactory areas can be prolonged by using viscous solutions or gels for nasal dosing; we can also use certain devices (e.g. insert a soft tube into the human nasal cavity to the olfactory areas) to apply the drug to the olfactory areas or let patients keep lying on their backs after i.n. administration.

The study conducted in rats clearly demonstrated effectiveness of intranasal delivery of tramadol and lamotrigine as antinociceptive agents. However, clinical data is needed to evaluate the risk vs. benefit ratio.

8.5 References

- Behl CR, Pimplaskar HK, Sileno AP, De Meireles J, Romeo VD. 1998. Effects of physicochemical properties and other factors on systemic nasal delivery. *Adv Drug Deliv Rev* 29: 89-116.
- Broadwell RD, Baker Cairns BJ, Friden PM, Oliver C, Villegas, JC. 1996. Transcytosis of protein through the mammalian cerebral epithelium and endothelium. III. Receptor-mediated transcytosis through the blood-brain barrier of blood-borne transferrin and antibody against the transferrin receptor. *Exp Neurol* 142:47– 65.
- Changa J, Jallouli Y, Kroubia M, Yuan X, Fengb W, Kangd C, Pud P, Betbedera D. 2009. Characterization of endocytosis of transferrin-coated PLGA nanoparticles by the blood-brain barrier. *Int J Pharm* 379:285–292.
- Debanne MT, Regoeczi E, Sweeney GD, Krestynski K. 1985. Interaction of human lactoferrin with the rat liver. *Am J Physiol* 248:G463-469.
- Fillebeen C, Descamps L, Dehouck MP, Fenart L, Benaïssa M, Spik G, Cecchelli R, Pierce A. 1999. Receptor-mediated transcytosis of lactoferrin through the blood-brain barrier. *J Biol Chem* 274:7011–7017.
- Fleming RE, Migas MC, Holden CC, Waheed A, Britton RS, Tomatsu S, Bacon BR, Sly WS. 2000. Transferrin receptor 2: continued expression in mouse liver in the face of iron overload and in hereditary haemochromatosis. *Proc Natl Acad Sci USA* 97:2214–2219.
- Hatakeyama H, Akita H, Maruyama K, Suhara T, Harashima H. 2004. Factors governing the in vivo tissue uptake of transferrin-coupled polyethylene glycol liposomes in vivo. *Int J Pharm* 281:25–33.
- Huang RQ, Ke W, Han L, Liu Y, Shao K, Jiang C, Pei YY. 2010. Lactoferrin-modified nanoparticles could mediate efficient gene delivery to the brain in vivo. *Brain Res Bull* 81:600–604.
- Huang RQ, Ke WL, Liu Y, Jiang C, Pei YY. 2008. The use of lactoferrin as a ligand for targeting the polyamidoamine-based gene delivery system to the brain. *Biomaterials* 29:238–246.
- Huang RQ, Ke WL, Qu YH, Zhu JH, Pei YY. 2007. Jiang C Characterization of lactoferrin receptor in brain endothelial capillary cells and mouse brain. *J Biomed Sci* 14:121–128.
- Illum, L. 2000. Transport of drugs from the nasal cavity to central nervous system. *Eur J Pharm Sci* 11: 1–18.

- Illum, L. 2003. Nasal drug delivery: problems, possibilities and solutions. *J Control Release* 87: 187-198.
- Jaeghere FD, Doelker E, gurny R. 1999. Encyclopedia of controlled drug delivery. In; John Wiley, ed., Nanoparticles. New York, USA. 2: 641-664.
- Jogani, V.V., Shah J.P., Mishra, P., Misra, A.K, Misra, A., 2008. Intranasal Mucoadhesive Microemulsion of Tacrine to Improve Brain Targeting. *Alzheimer Dis Assoc Disord* 22(2):116-24.
- Jung BH, Chung BC, Chung S, Shim C. 2000. Prolonged delivery of nicotine in rats via nasal administration of proliposomes. *J Contol Release* 66: 73-79.
- Kawabata H, Germain RS, Ikezoe T, Tong X, Green EM, Gombart AF, Koeffler HP. 2001. Regulation of expression of murine transferrin receptor 2. *Blood* 98:1949–1954.
- Lawrence MJ, Rees GD. 2000. Microemulsion based media as novel drug delivery system. *Adv Drug Delivery Rev* 45: 89- 121.
- Lianli L, Nandi I and Kim KH. 2002. Development of an ethyl laurate-based microemulsion for rapid-onset intranasal delivery of diazepam. *Int J Pharmaceutics* 237(1-2): 77-85.
- Litzinger DC, Buiting AM, Van Rooijen N, Huang L. 1994. Effect of liposome size on the circulation time and intra organ distribution of amphipathic poly (ethylene glycol)-containing liposomes. *Biochem Biophys Acta* 1190:99–107.
- Moghimi SM, Hedeman H, Muir IS, Illum L, Davis SS. 1993. An investigation of the filtration capacity and the fate of large filtered sterically-stabilized microspheres in rat spleen. *Biochim Biophys Acta* 1157:233–240.
- Sahoo SK, Labhasetwar V. 2005. Enhanced Antiproliferative Activity of Transferrin-Conjugated Paclitaxel-Loaded Nanoparticles Is Mediated via Sustained Intracellular Drug Retention. *Mol Pharmaceutics* 2:373-383.
- Stolnik S, Heald CR, Neal J, Garnett MC, Davis SS, Illum L, Purkis SC, Barlow RJ, Gellert PR. 2001. Polylactide-poly(ethylene glycol) micellar-like particles as potential drug carriers: Production, colloidal properties and biological performance. *J Drug Targeting* 9:361–378.
- Suzuki YA, Lonnerdal B. 2002. Characterization of mammalian receptors for lactoferrin. *Biochem Cell Biol* 80:75– 80.
- Talukder MJ, Takeuchi T, Harada E. 2003. Receptor-mediated transport of lactoferrin into the cerebrospinal fluid via plasma in young calves. *J Vet Med Sci* 65:957–964.

- Thorne RG, Pronk GJ, Padmanabhan V, Frey WH 2nd. 2004. Delivery of insulin-like growth factor-I to the rat brain and spinal cord along olfactory and trigeminal pathways following intranasal administration. *Neuroscience* 127(2): 481-496.
- Vyas TK, Babbar AK, Sharma RK, Misra A. 2005. Intranasal mucoadhesive microemulsions of zolmitriptan: Preliminary studies on brain-targeting. *J Drug Targeting* 13(5): 317-324.
- Zhang Q, Jiang X, Xiang W, Lu W, Su L, Shi Z. 2004. Preparation of nimodipine-loaded microemulsion for intranasal delivery and evaluation of the targeting efficiency to brain. *Int J Pharm* 275: 85-96.
- Zhao Y, Yue P, Tao T, Chen QH. 2007. Drug brain distribution following intranasal administration of Huperzine A insitu gel in rats. *Acta Pharmacologica sinica* 28(2): 273-278.
- Ziere GJ, van Dijk MC, Bijsterbosch MK, van Berkel TJ. 1992. Lactoferrin uptake by the rat liver: Characterization of the recognition site and effect of selective modification of arginine residues. *J Biol Chem* 267:11229-11235.